

UNCLASSIFIED



3 4456 0360891 4

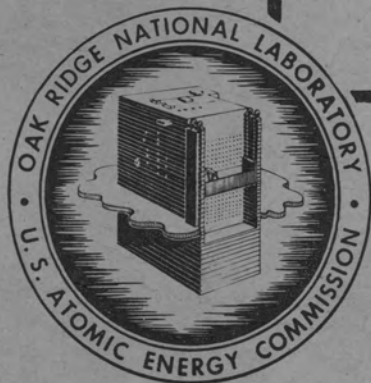
ORNL-1092  
Progress Report  
*9a*

**PHYSICS DIVISION**  
**QUARTERLY PROGRESS REPORT**  
**FOR PERIOD ENDING JUNE 20, 1951**

**CENTRAL RESEARCH LIBRARY**  
**DOCUMENT COLLECTION**  
**LIBRARY LOAN COPY**

**DO NOT TRANSFER TO ANOTHER PERSON**

If you wish someone else to see this document,  
send in name with document and the library will  
arrange a loan.



**OAK RIDGE NATIONAL LABORATORY**  
OPERATED BY  
**CARBIDE AND CARBON CHEMICALS COMPANY**  
A DIVISION OF UNION CARBIDE AND CARBON CORPORATION



POST OFFICE BOX P  
OAK RIDGE, TENNESSEE

UNCLASSIFIED

**UNCLASSIFIED**

**ORNL-1092**

This document consists of 55 pages.

Copy 9 of 318. Series A.

Contract No. W-7405, eng 26

**PHYSICS DIVISION**

A. H. Snell, Director  
E. O. Wollan, Associate Director

**QUARTERLY PROGRESS REPORT**

**for Period Ending June 20, 1951**

Edited by:

L. D. Roberts

DATE ISSUED: ~~JUN~~ 27 1951

**OAK RIDGE NATIONAL LABORATORY**  
operated by  
**CARBIDE AND CARBON CHEMICALS COMPANY**  
A Division of Union Carbide and Carbon Corporation  
Post Office Box P  
Oak Ridge, Tennessee

**UNCLASSIFIED**



3 4456 0360891 4

# UNCLASSIFIED

## DISTRIBUTION

ORNL-1092  
Progress Report

### INTERNAL DISTRIBUTION

- |        |                         |        |                      |
|--------|-------------------------|--------|----------------------|
| 1.     | G. T. Felbeck (C&CCC)   | 34.    | J. A. Lane           |
| 2-3.   | Chemistry Library       | 35.    | R. N. Lyon           |
| 4.     | Physics Library         | 36.    | W. C. Koehler        |
| 5.     | Biology Library         | 37.    | W. K. Ergen          |
| 6.     | Health Physics Library  | 38.    | E. P. Blizard        |
| 7.     | Metallurgy Library      | 39.    | M. E. Rose           |
| 8-9.   | Training School Library | 40.    | G. E. Boyd           |
| 10-13. | Central Files           | 41.    | Lewis Nelson         |
| 14.    | C. E. Center            | 42.    | R. W. Stoughton      |
| 15.    | C. E. Larson            | 43.    | C. E. Winters        |
| 16.    | W. B. Humes (K-25)      | 44.    | W. H. Jordan         |
| 17.    | W. D. Lavers (Y-12)     | 45.    | E. C. Campbell       |
| 18.    | A. M. Weinberg          | 46.    | D. S. Billington     |
| 19.    | E. H. Taylor            | 47.    | M. A. Bredig         |
| 20.    | E. D. Shipley           | 48.    | R. S. Livingston     |
| 21.    | E. J. Murphy            | 49.    | C. P. Keim           |
| 22.    | F. C. VonderLage        | 50.    | J. L. Meem           |
| 23.    | A. H. Snell             | 51.    | C. E. Clifford       |
| 24.    | J. A. Swartout          | 52.    | G. H. Clewett        |
| 25.    | A. Hollaender           | 53.    | C. D. Susano         |
| 26.    | K. Z. Morgan            | 54.    | C. J. Borkowski      |
| 27.    | F. L. Steahly           | 55.    | M. J. Skinner        |
| 28.    | M. T. Kelley            | 56.    | L. A. Rayburn        |
| 29.    | E. M. King              | 57.    | S. Bernstein         |
| 30.    | E. O. Wollan            | 58.    | P. M. Reyling        |
| 31.    | D. W. Cardwell          | 59.    | D. D. Cowen          |
| 32.    | A. S. Householder       | 60-75. | Central Files (O.P.) |
| 33.    | L. D. Roberts           |        |                      |

### EXTERNAL DISTRIBUTION

- 76. American Cyanamid Company
- 77-84. Argonne National Laboratory
- 85. Armed Forces Special Weapons Project
- 86-91. Atomic Energy Commission - Washington
- 92. Battelle Memorial Institute
- 93. Brush Beryllium Company
- 94-97. Brookhaven National Laboratory
- 98. Bureau of Medicine and Surgery
- 99. Bureau of Ships

# UNCLASSIFIED

ORNL-1092  
Progress Report

- 100-101. Carbide and Carbon Chemicals Company (C-31), Paducah
- 102-105. Carbide and Carbon Chemicals Company (K-25)
- 106-109. Carbide and Carbon Chemicals Company (Y-12)
  - 110. Columbia University (Failla)
  - 111. Columbia University (Havens)
- 112-116. Du Pont de Nemours and Company
- 117-118. Eldorado Mining and Refining Ltd.
- 119-121. General Electric Company, Richland
- 122-125. Idaho Operations Office
- 126-127. Iowa State College
  - 128. Kansas City Operations Branch
- 129-130. Kellex Corporation
- 131-132. Kirtland Air Force Base
- 133-136. Knolls Atomic Power Laboratory
- 137-139. Los Alamos Scientific Laboratory
  - 140. Mallinckrodt Chemical Works
  - 141. Massachusetts Institute of Technology (Kaufmann)
- 142-144. Mound Laboratory
  - 145. National Advisory Committee for Aeronautics
  - 146. National Bureau of Standards (Taylor)
  - 147. Naval Medical Research Institute
- 148-149. Naval Radiological Defense Laboratory
  - 150. New Brunswick Laboratory
- 151-153. New York Operations Office
  - 154. North American Aviation, Inc.
  - 155. Patent Branch, Washington
  - 156. Rand Corporation
  - 157. Sandia Corporation
  - 158. Savannah River Operations Office
- 159-233. Technical Information Service, Oak Ridge
- 234-239. USAF, Major James L. Steele
- 240-241. U. S. Geological Survey
- 242-243. U. S. Public Health Service
  - 244. University of California at Los Angeles
- 245-249. University of California Radiation Laboratory
- 250-251. University of Rochester
  - 252. University of Washington
  - 253. Western Reserve University
- 254-257. Westinghouse Electric Corporation
- 258-261. Atomic Energy Project, Chalk River (The Library)
  - 262. Gregory Breit (Sloane Physics Laboratory)
  - 263. Carnegie Institute of Technology (E. Creutz)
  - 264. Chief of Naval Research
  - 265. H. K. Ferguson Company (Miss Dorothy M. Lasky)
  - 266. Harshaw Chemical Company (Mr. K. E. Long)

UNCLASSIFIED

# UNCLASSIFIED

ORNL-1092  
Progress Report

- 267. Isotopes Division (Mr. J. A. McCormick)
- 268-269. Library of Congress (Alton H. Keller)
- 270. National Bureau of Standards (The Library)
- 271. National Research Council, Ottawa (Mr. J. M. Manson)
- 272-286. Naval Research Laboratory (Code 2028)
- 287-288. Nevis Cyclotron Laboratories (Mr. M. W. Johnson)
- 289-290. Oak Ridge Institute of Nuclear Studies (Mr. R. A. Schlueter)
- 291-300. United Kingdom Scientific Mission
- 301-305. USAF, Central Air Documents Office (CADO-E)
- 306. USAF, Director of Research & Development (Research Division)
- 307. USAF, Wright-Patterson Air Force Base (Colonel Leo V. Harman)
- 308. U. S. Army, Army Field Forces (CWO Edwin H. Hoffman)
- 309. U. S. Army, Army Medical Service Graduate School  
(Col. W. S. Stone)
- 310-312. U. S. Army, Chemical and Radiological Laboratories (Miss Amoss)
- 313. U. S. Army, Director of Operations Research Office  
(E. Johnson)
- 314. U. S. Army, Office, Chief of Ordnance (Col. A. R. Del Campo)
- 315-316. U. S. Army, Office of the Chief Signal Officer (Mr. N. Stulman  
thru Lt. Col. G. C. Hunt)
- 317. U. S. Army, Special Weapons Branch (Lt. Col. A. W. Betts)
- 318. UT-AEC Agricultural Research Program (C. L. Comar)

# UNCLASSIFIED

Physics Division quarterly progress reports previously issued in this series are as follows:

ORNL-325 Supplement	December, January, and February, 1948-49
ORNL-366	Period Ending June 15, 1949
ORNL-481	Period Ending September 25, 1949
ORNL-577	Period Ending December 15, 1949
ORNL-694	Period Ending March 15, 1950
ORNL-782	Period Ending June 15, 1950
ORNL-865	Period Ending September 20, 1950
ORNL-940	Period Ending December 20, 1950
ORNL-1005	Period Ending March 20, 1951

UNCLASSIFIED

# UNCLASSIFIED

## TABLE OF CONTENTS

	PAGE NO.
INTRODUCTION AND SUMMARY	1
PUBLICATIONS	4
1. NEUTRON DIFFRACTION	5
The Neutron Coherent Scattering Cross-Section of $C^{13}$	5
Neutron-Diffraction Studies of Antiferromagnetism	7
2. SHORT-LIVED ISOMERS	11
3. INTERACTION OF LOW-ENERGY IONS WITH SOLIDS AND GASES	15
Ion Source Studies	15
Detection of Positive Ion Beam	15
Gas-Scattering Apparatus	15
Bombardment of Thin Surface Films	16
4. HIGH VOLTAGE PROGRAM	17
Neutron Cross-Sections	17
Thick target $(p, n)$ yields	17
The $Be^9(p, n)B^9$ yield	17
5 Mv machine calibration and performance	17
Gamma-Ray Spectroscopy	18
Capture gamma rays from protons on $N^{14}$	18
Charged Particle Reactions	21
The reaction of $He^3 + He^3$	21
5. SHORT-PERIOD ACTIVITIES	24
Double-Channel Coincidence Spectrometer	24
6. HARD GAMMA EMITTERS AMONG FISSION FRAGMENTS	27
7. TIME-OF-FLIGHT SPECTROMETER	29
8. INVESTIGATIONS WITH THE SCINTILLATION SPECTROMETER	30
$I^{131}$ Gamma Rays	30
Hollow-Crystal Spectrometer	30
Improvement of Resolution of Scintillation Spectrometers	32
High-Speed Synchroscope	38
Blue Glow from LITR	38

# UNCLASSIFIED

	PAGE NO.
9. THEORETICAL PHYSICS	41
L-Shell Internal Conversion	41
Angular Correlation with Conversion Electrons	41
Polarization of Capture Gamma Radiation	41
Isotropy of Nuclear Gamma Radiation	42
Angular Correlation in Beta Decay	42
The General Beta-Decay Interaction	42
Effect of Finite Size of Nucleus in Beta Decay	43
Nuclear Alignment	43
On the Stopping Power for Fission Fragments	43
Tabulation of the Racah Coefficients	43
The Triplet Force Between Like Nucleons	44

UNCLASSIFIED

# UNCLASSIFIED

## LIST OF TABLES

TABLE NO.	TITLE	PAGE NO.
1	Parameters of $\text{BaCO}_3$ Based on $P(b, n, m)$ with $x = a_0$ , $y = b_0$ , $c = z_0$	6
2	Calculated Structure Factors for Barium Carbonate	7
3	Nuclei Investigated for Short-Lived Isomers	11
4	Some Measured Internal Conversion Coefficients in the K-Shell	13
5	Hard Gamma Emitters Among Fission Fragments	27

# UNCLASSIFIED

## LIST OF FIGURES

FIGURE NO.	TITLE	PAGE NO.
1	Effective Carbon Scattering Amplitudes	8
2	Experimental Values of $F_{100}^2$ for $\text{MnF}_2$	9
3	Experimental Values of $F_{100}^2$ for $\text{FeF}_2$	9
4	Experimental Values of $F_{100}^2$ for $\text{NiF}_2$	9
5	Low-Energy $\gamma$ -Ray Spectrum from $\text{Ho}^{166} \xrightarrow[27 \text{ hr}]{\beta^-} \text{Er}^{166}$	12
6	Low-Energy $\gamma$ -Ray Spectrum from $\text{Ho}^{166} \xrightarrow[27 \text{ hr}]{\beta^-} \text{Er}^{166}$ Resolved into Gaussian Components	12
7	Thick Target ( $p, n$ ) Yield Curves Measured with Bonner Type Counter	18
8	$\text{Be}^9(p, n)\text{B}^9$ Yield Curve Measured with Long Counter	19
9	Gamma Rays from $\text{N}^{14}(p, \gamma)$ Reaction	20
10	Energy Distribution of Protons from Bombarding $\text{He}^3$ on Clean Aluminum	22
11	Double Channel Coincidence Spectrometer	25
12	$\text{I}^{131}$ $\gamma$ Rays Using NaI Crystal (5/23/51)	31
13	Hollow Crystal Spectrometer	32
14	$\text{Ca}^{45}$ Collimated by .030-in. Copper Sheet on Hollow Anthracene Spectrometer	33
15	Kurie Plot of $\text{Ca}^{45}$ Using Copper Collimator on Hollow Anthracene Spectrometer	34
16	Transmission Spectra of Substances Used on Scintillation Spectrometry	35
17	Transmission Spectra of Various Crystals and Solutions	36
18	Emission Spectra of Anthracene and Sodium Iodide Activated with Thallium	37



# UNCLASSIFIED

## INTRODUCTION AND SUMMARY

This report covers unclassified work of the Physics Division for the period March 20, 1951 to June 20, 1951. The classified section of the Physics Division quarterly report appears separately (ORNL-1107).

Additions to the research staff in the Physics Division during this quarter are: Dr. C. H. Johnson (High Voltage Program); Dr. W. K. Ergen, Dr. Samuel Podgor, Mr. Keith Henry, Mr. Francis Muckenthaler, and Dr. Fred Maienschein (Bulk Shielding Program); Dr. Conway Snyder, Mr. Francis Green, and Mr. Joe Bair (5-Mev Van de Graaff Group); Mr. Eugene Haake (ANP Critical Experiments Program).

The following persons have spent the summer months working in the Physics Division under the Research Participation Program: Dr. D. S. Hughes, University of Texas (Scintillation Spectrometer); Dr. C. C. Sartain, University of Alabama (Low Temperature); Dr. T. M. Hahn, University of Kentucky (5-Mev Van de Graaff); Dr. J. M. Jauch, Iowa State University (Theoretical Group); Dr. W. E. Millett, University of Mississippi (Scintillation Spectrometer); Dr. H. C. Thomas, Vanderbilt University (Scintillation Spectrometer); Dr. D. B. Beard, Catholic University (Theoretical Group); Mr. R. H. Rohrer, Duke University (Special Assignment).

The following students from Cornell University have spent the summer working in the Physics Division: Messrs. Walter A. Harrison, Frank Loeffler, and James W. Schwartz.

**Neutron Diffraction.** From neutron-diffraction measurements on two samples

of barium carbonate enriched in  $C^{13}$ , the scattering amplitude of  $C^{13}$  has been determined to be positive with the magnitude  $0.65 \pm 0.03 \times 10^{-12}$  cm. Structure factors for a few of the reflections of barium carbonate have been tabulated.

Ferrous fluoride and cobaltous fluoride have been found to give superlattice neutron-diffraction peaks due to an ordered electron-spin structure in the temperature region 10 to 77°K. The temperature dependence of the intensity of the 100 superlattice diffraction peak has been measured and a theory for this dependence is proposed. The measurements are found to compare well with this theory for the three fluorides studied, manganous fluoride, ferrous fluoride, and nickelous fluoride.

**Short-Lived Isomers.** The radiation announcing the formation of an excited state in  $Dy^{160}$  with a half-life of  $1.8 \pm 0.2 \times 10^{-9}$  sec and the radiation resulting from its decay have been studied. The upper limits for the half-life of excited states for  $Te^{123}$ ,  $Te^{125}$ ,  $Ho^{165}$ ,  $Hg^{198}$ , and  $Tl^{203}$  are found to be in the range  $4 \times 10^{-10}$  sec to  $20 \times 10^{-10}$  sec. The corresponding  $\gamma$ -ray energies are given. The K-shell internal conversion coefficients have been measured for  $Dy^{160}$ ,  $Ho^{165}$ ,  $Er^{166}$ , and  $Yb^{170}$ .

**Interaction of Low-Energy Ions with Solids and Gases.** A PIG type ion source operating at a low gas pressure and power consumption has yielded stable heavy ion beams up to 400  $\mu$ a. Apparatus is being set up to accelerate these beams to an energy in the range

# UNCLASSIFIED

## PHYSICS DIVISION QUARTERLY REPORT

from 20 to 400 Kev for study of their interaction with gases and solids.

**High Voltage Program.** A High Voltage Corporation 5-Mev Van de Graaff generator has recently been installed and is being adapted for neutron work. In connection with reducing the neutron background from the machine, thick target  $(p,n)$  yields have been measured for tantalum, tungsten, molybdenum, and brass in the energy region from 2.2 to 5.4 Mev. The  $\text{Be}^9(p,n)\text{B}^9$  yield has been measured as a function of energy from the threshold at  $2.059 \pm .002$  Mev to 5.1 Mev. A new resonance was found at about 4.5 Mev.

Using a Cockcroft-Walton generator, the  $\gamma$ -ray spectrum resulting from the resonance capture of 277-Kev protons by  $\text{N}^{14}$  has been studied. Six  $\gamma$  rays from  $\text{O}^{15}$  are found. These can be correlated with the previously measured total excitation energy of the reaction only if three intermediate levels of  $\text{O}^{15}$  are assumed.

Preliminary results on the capture of 300-Kev  $\text{He}^3$  nuclei by  $\text{He}^3$  have been obtained. The most likely reaction is  $\text{He}^3 + \text{He}^3 \longrightarrow \text{He}^4 + \text{H}^1 + \text{H}^1 + 12.82$  Mev.

**Short-Period Activities.** A pulse height analyzer capable of measuring the height of each of two coincident pulses has been developed using a cathode ray oscilloscope display technique.

**Hard-Gamma Emitters Among Fission Fragments.** The photon-neutron yield in deuterium and beryllium from  $\gamma$  rays produced by neutron irradiated  $\text{U}^{235}$  has been correlated with the known properties of the fission product  $\gamma$  rays.

**Time-of-Flight Spectrometer.** A rotating shutter time-of-flight neutron spectrometer for the measurement of total neutron cross-sections at energies up to 5 Kev is under construction.

**Investigations with the Scintillation Spectrometer.** New coincidence spectrometer measurements of  $\text{I}^{131}$  with improved resolution have been made and a previously unknown  $\gamma$  ray of about 0.5 Mev energy has been detected. This new  $\gamma$  ray does not fit the previously accepted  $\text{I}^{131}$  decay scheme.

The development of the hollow-crystal spectrometer has been continued and the instrument has been used for the study of the  $\beta$  radiation of  $\text{Ca}^{45}$ . It is now being used to study the  $\beta$ - $\gamma$  coincidence spectrum of  $\text{I}^{131}$ .

As a result of studies of the optical absorption of samples of anthracene, sodium iodide, mineral oil, and Canada balsam in the wave length range from 3200 to 5500 A, the resolution of the scintillation spectrometer has been much improved. Further improvements have been made by suitable treatment of the optical surfaces of the spectrometer. A new synchroscope with a vertical amplifier rise time of about 1  $\mu\text{sec}$  is in process of development for study of circuits and components to be used in very fast counting equipment and for the investigation of various discharge phenomena.

The bluish white glow emitted by water immediately surrounding an intensely radioactive uranium slug has been identified as Cerenkov radiation.

**Theoretical Physics.** The nature and status of the problems of current

# UNCLASSIFIED

FOR PERIOD ENDING JUNE 20, 1951

interest to the theoretical physics group are summarized below.

1. The calculations of L-shell internal conversion coefficients is being carried out in Washington on the Bureau of Standards machine (SEAC).

2. A method has been developed to obtain the angular correlation for conversion of electrons with  $\gamma$  rays,  $\beta$  particles,  $\alpha$  particles, and also the conversion electron--conversion electron correlation.

3. It has been shown that the capture  $\gamma$  rays resulting from the capture of polarized neutrons by nuclei exhibit anisotropy to a detector which can discriminate between right and left circular polarization.

4. In order that the  $B^{11}(p,\gamma)C^{12}$  reaction can be explained, it is postulated that two levels of the  $C^{12}$  nucleus are reached. The theory is discussed. In particular, it has been demonstrated, in general, that if a  $2^L$  pole  $\gamma$  ray is emitted isotropically and  $L \geq J - \frac{1}{2}$  where  $J$  is the angular momentum of the emitting level, then all gamma radiation from this level must be isotropic.

5. The  $\beta$ - $x$  angular correlation, where  $x$  is any radiation, has previously been calculated in the  $Z = 0$  approximation. This work is being extended by including the Coulomb field.

6. The most general  $\beta$  decay interaction is discussed.

7. The effect of the finite size of the nucleus in  $\beta$  decay is discussed.

8. The degree of nuclear alignment produced by HFS coupling is shown to be independent of the degree of magnetic dilution of the paramagnetic salt used.

9. The effect of screening by the orbital electrons on the slowing down of fission fragments has been investigated.

10. Progress has been made in the tabulation of the Racah coefficients. The tables currently completed are listed.

11. The forces, the triplet force in particular, between like nucleons are discussed.

UNCLASSIFIED

# UNCLASSIFIED

## PHYSICS DIVISION QUARTERLY REPORT

### PUBLICATIONS

A list of publications by the Physics Division during the past quarter is as follows:

1. S. Tamor\*, "The Absorption of Slow  $\pi^-$  Mesons in Deuterium," *Phys. Rev.* **82**, 38-43 (1951).
2. L. Biedenharn, "A Note on Time Reversal and the Dirac Equation," *Phys. Rev.* **82**, 100 (1951).
3. P. R. Bell, Judith M. Cassidy, and G. G. Kelley, "The Disintegration Scheme of  $I^{131}$ ," *Phys. Rev.* **82**, 103 (1951).
4. John M. Blatt\*\* and Lawrence C. Biedenharn, "The Angular Dependence of Scattering and Reaction Cross Sections," *Phys. Rev.* **82**, 123 (1951).
5. M. E. Rose, "A Note on Dirac Central Field Wave Functions," *Phys. Rev.* **82**, 389-391 (1951).
6. M. E. Rose and R. R. Newton, "Properties of Dirac Wave Functions in a Central Field," *Phys. Rev.* **82**, 470-477 (1951).
7. Max Goodrich, "Radiation of  $Ag^{110}$ ," *Phys. Rev.* **82**, 759-760 (1951).
8. L. C. Biedenharn and M. E. Rose, "The Relative Phase of the Interaction Constants for Mixed Invariants in Beta-Decay," *Phys. Rev.* **83**, 459 (1951).

\*Work done while an AEC predoctoral fellow.

\*\*University of Illinois.

# UNCLASSIFIED

FOR PERIOD ENDING JUNE 20, 1951

## 1. NEUTRON DIFFRACTION

### THE NEUTRON COHERENT SCATTERING CROSS-SECTION OF $C^{13}$

E. O. Wollan      C. G. Shull  
W. C. Koehler

Normal carbon contains 98.9%  $C^{12}$ , a zero spin isotope, and 1.1%  $C^{13}$ . Disregarding the small isotopic impurity, carbon is essentially a single, zero-spin nuclide, and as such is useful as a standard scatterer in neutron-diffraction measurements. The calculation of a coherent scattering cross-section from transmission studies of monoisotopic zero-spin nuclei is simplified because of the absence of isotopic or spin incoherent scattering, and hence such measurements, combined with neutron-diffraction patterns, permit the calibration of the intensities of Bragg-scattered neutrons by powdered crystals in terms of absolute units. In order to establish the effect of the 1.1% of  $C^{13}$  in normal carbon, neutron-diffraction studies have been made on  $BaCO_3$  enriched in  $C^{13}$ .

Two isotopically enriched samples, 53 and 40 atom %  $C^{13}$ , originally prepared by the Eastman Kodak Company, were kindly loaned to us by Dr. S. F. Carson of the ORNL Biology Division. Neutron-diffraction patterns of these samples and also of normal  $BaCO_3$  were obtained.

Barium carbonate (witherite) is orthorhombic with four molecules per unit cell. It is isomorphous with  $KNO_3$  and with several divalent metal carbonates, the prototype of which is

aragonite ( $CaCO_3$ ). Wyckoff<sup>(1)</sup> gives the space group as  $V_h^{16} = P(b,n,m)$  with  $a_0 = 8.8345$  A,  $b_0 = 6.5490$  A, and  $c_0 = 5.2556$  A. The barium, carbon, and four of the oxygen atoms are in special positions of the space group, while the remaining eight oxygens occupy general positions. Barium parameters were reported by Zachariasen,<sup>(2)</sup> and Colby and LaCoste<sup>(3)</sup> have described the complete structure.

Structure factors have been calculated on the parameters given in Table 1 and with the bound scattering amplitudes of oxygen and barium taken to be  $0.580 \times 10^{-12}$  cm and  $0.528 \times 10^{-12}$  cm, respectively.<sup>(4,5)</sup> The structure factors have been calculated in units of  $10^{-12}$  cm per unit cell and have been expressed in terms of the carbon scattering amplitude wherever it has a finite contribution to the line. In Table 2 structure factors for a few of the reflections of  $BaCO_3$  have been tabulated. In spite of the fact that the symmetry is low, it is possible in this case to obtain a quantitative measure of the carbon scattering amplitude. In the diffraction patterns

---

(1) R. W. G. Wyckoff, *Crystal Structures*, Interscience, 1948.

(2) W. H. Zachariasen, "Untersuchungen über die Kristallstruktur von Sesquioxiden und Verbindungen  $ABO_3$ ," *Skrifter Norske Videnskaps-Akad. Oslo. I, Matemat. Naturv. Klasse*, No. 4, p. 1 (1928).

(3) M. Y. Colby and L. J. B. LaCoste, "The Crystal Structure of Witherite," *Z. Krist.* 90, 1 (1935).

(4) C. G. Shull and E. O. Wollan, "Coherent Scattering Amplitudes as Determined by Neutron Diffraction," *Phys. Rev.* 81, 527 (1951).

(5) C. G. Shull, E. O. Wollan, and W. C. Koehler, "Neutron Diffraction," *Physics Division Quarterly Progress Report for Period Ending March 20, 1951*, ORNL-1005, p. 13 (July 24, 1951).

UNCLASSIFIED

# UNCLASSIFIED

## PHYSICS DIVISION QUARTERLY REPORT

TABLE 1

Parameters of  $\text{BaCO}_3$  Based on  $P(b, n, m)$  with  $x = a_0$ ,  $y = b_0$ ,  $c = z_0$

Ba, C,  $O_I$  in  $\pm (u, v, \frac{1}{4}; \frac{1}{2} - u, v + \frac{1}{2}, \frac{1}{4})$

$O_{II}$  in  $\pm (x, y, z; x, y, \frac{1}{2} - z; \frac{1}{2} - x, \frac{1}{2} + y, z; \frac{1}{2} - x, \frac{1}{2} + y, \frac{1}{2} - z)$

	x = a <sub>0</sub>	y = b <sub>0</sub>	z = c <sub>0</sub>
Ba	150°	270.8°	90°
C	270°	-34°	90°
O <sub>I</sub>	320°	-34°	90°
O <sub>II</sub>	245°	-34°	163°

The description of the structure on which the parameters of Table 1 are based differs from that adopted by Colby and LaCoste and from that of descriptive crystallography. Colby and LaCoste have based their discussions on positions 4(c) and 8(d) of  $V_h^{16}$  of Wyckoff's "Analytical Expression of the Results of the Theory of Space Groups": If  $x'$ ,  $y'$ ,  $z'$  represent the coordinates of Colby and LaCoste, and  $x$ ,  $y$ ,  $z$  those given in the table, then  $x' = z - \frac{1}{4}$ ,  $y' = y + \frac{1}{4}$ , and  $z' = x$ , with  $x' = a = 5.2556$  A,  $y' = c = 6.5490$  A, and  $z' = b = 8.8345$  A.

of all three samples, the first three reflections appear as a single peak but nicely resolved from the remainder of the pattern. Of these first three lines, the first is very weak, and the other two show a strong carbon contribution.

The intensity of this first composite peak (110, 101, 200) in each of the three samples was evaluated in terms of the coherent scattering cross-section of 13.4 barns for nickel. A rough estimate of the characteristic temperatures of  $\text{BaCO}_3$  was made, and the intensities were corrected upward

by 2 percent to take account of the effects of lattice vibrations. From the observed intensities the effective scattering amplitude of carbon in each of the three isotopic mixtures was evaluated. Since the intensity of the scattered beam depends upon the square of the structure factor, and hence is quadratic in  $f_C$ , two roots, one positive and one negative, were obtained from each sample. An estimate of the errors involved in the experimental determination of intensities and in the sensitivity of the structure factors to the light atom positions was made, and the results are shown in Fig. 1.

# UNCLASSIFIED

FOR PERIOD ENDING JUNE 20, 1951

TABLE 2

Calculated Structure Factors for Barium Carbonate

INDEX	F /UNIT CELL	SCATTERING ANGLE	F  <sup>2</sup> /(UNIT CELL) <sup>2</sup>
100	0		0
010	0		0
110	$.0484f_{Ba} - 0.262f_o$	11.24	0.0160
001	0		0
101	$4f_c + 4.69f_o - 2f_{Ba}$	13.10	$16f_c^2 + 13.3f_c + 2.77$
200	$4f_c + 4.45f_o - 2f_{Ba}$	13.40	$16f_c^2 + 12.2f_c + 2.32$
011	0		0
111	$3.46f_{Ba} - 1.15f_o$	15.92	1.36
210	$3.46f_{Ba} - 1.12f_o$	16.16	1.39
201	0		0
020	$-3.98f_{Ba} + 1.50f_o + 4.49f_o$	18.10	$2.24f_c^2 + 1.52f_c + 0.257$
120	$-.0558f_{Ba} + 3.71f_c + 9.105f_o$	19.32	$13.8f_c^2 + 38.9f_c + 27.6$

The lines in the figure correspond only to the positive root for

$$f_c = (p_1 f_{12} + p_2 f_{13})$$

where  $p_1$  is the fraction of  $C^{12}$ ,  $p_2$  is the fraction of  $C^{13}$ , and  $f_{12}$  and  $f_{13}$  are the scattering amplitudes of the two isotopes. The negative roots are excluded because the scattering amplitude of normal carbon is known to be positive.<sup>(4)</sup> Hence the scattering amplitude of  $C^{13}$  is uniquely determined to be positive with the magnitude  $0.65 \pm 0.03 \times 10^{-12}$  cm. Clearly the

isotopic incoherence to be expected from normal carbon due to the presence of 1.1%  $C^{13}$  is negligible.

## NEUTRON-DIFFRACTION STUDIES OF ANTIFERROMAGNETISM

R. A. Erickson

Neutron-diffraction studies of anti-ferromagnetism in some iron group compounds having the  $SnO_2$  tetragonal structure have been undertaken. These consist of  $MnF_2$ ,  $FeF_2$ ,  $CoF_2$ ,  $NiF_2$ , and  $MnO_2$ . This body-centered structure seems of particular interest because of

# UNCLASSIFIED

## PHYSICS DIVISION QUARTERLY REPORT

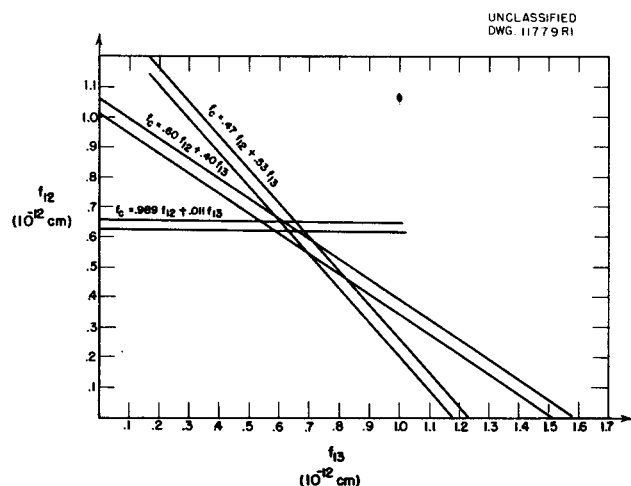


Fig. 1 - Effective Carbon Scattering Amplitudes.

its close resemblance to the two-sublattice model used by Van Vleck<sup>(6)</sup> in his theory of antiferromagnetism.

It was previously reported<sup>(7)</sup> that neutron-diffraction patterns on  $MnF_2$

and  $NiF_2$  show that below a critical temperature these compounds begin to assume an ordered magnetic structure in which the magnetic moments of the ions at the body-center and corner positions are coupled antiparallel. This ordering is evidenced by a progressive decrease in the paramagnetic diffuse scattering and the simultaneous growth of superlattice diffraction peaks as the temperature is reduced. In more recent measurements  $FeF_2$  and  $CoF_2$  have been found to behave similarly.

For this structure the temperature variation of the intensity in the diffraction peaks should be approximately described by combining Van Vleck's<sup>(6)</sup> results for the thermal dependence of the spontaneous magnetization of a simple antiferromagnetic lattice with those of Halpern and Johnson<sup>(8)</sup> for the scattering resulting from the magnetic interaction between a neutron and a paramagnetic ion. This is

$$F_{hkl}^2 = 4 \left[ \frac{e}{\hbar c} \gamma g S B_s(y) (f_e q)_{hkl} \right] \left. \begin{array}{l} h + k + 1 \text{ odd} \\ h + k + 1 \text{ even} \end{array} \right\} = 0 \quad (1)$$

where

$$y = 3B_s(y) \frac{s}{s+1} \frac{T_c}{T},$$

(6) J. H. Van Vleck, "On the Theory of Antiferromagnetism," *J. Chem. Phys.* 9, 85 (1941).

(7) R. A. Erickson, "Magnetic Structure of  $MnF_2$  and  $NiF_2$ ," ORNL-1005, *op. cit.*, p. 14.

(8) O. Halpern and M. H. Johnson, "On the Magnetic Scattering of Neutrons," *Phys. Rev.* 55, 898 (1939).

# UNCLASSIFIED

FOR PERIOD ENDING JUNE 20, 1951

$F_{hkl}$  is the crystalline structure factor for magnetic scattering from the  $hkl$  planes,  $\gamma$  is the neutron magnetic moment in nuclear Bohr magnetons,  $gSB$  is the effective magnetic moment (for neutron scattering) of the paramagnetic ion of electron spin  $S$ ,  $B_s(\gamma)$  is the Brillouin function,  $T_c$  is the curie temperature,  $f_e$  is the magnetic form factor of the ion corresponding to the spatial distribution of 3d electrons, and  $q$  is equal in magnitude to the sine of the angle between the scattering vector and the direction of spontaneous magnetization.

The experimental values of  $F_{100}^2$  for  $MnF_2$ ,  $FeF_2$ , and  $NiF_2$  are shown in Figs. 2-4. These are compared with

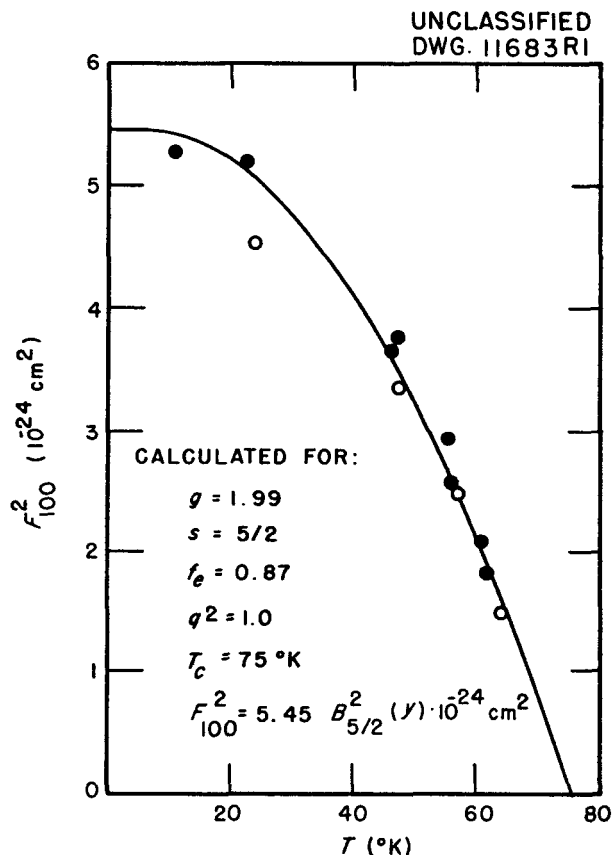


Fig. 2 - Experimental Values of  $F_{100}^2$  for  $MnF_2$ .

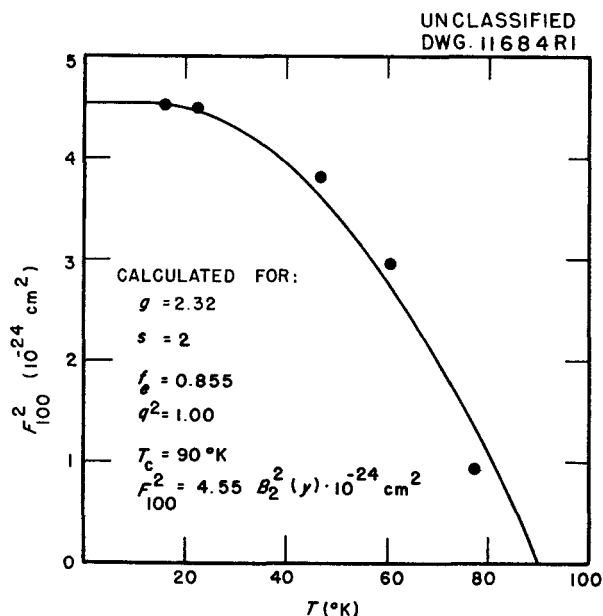


Fig. 3 - Experimental Values of  $F_{100}^2$  for  $FeF_2$ .

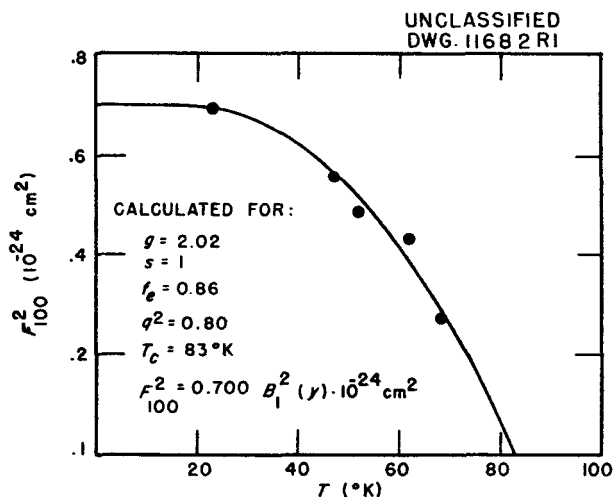


Fig. 4 - Experimental Values of  $F_{100}^2$  for  $NiF_2$ .

# UNCLASSIFIED

## PHYSICS DIVISION QUARTERLY REPORT

expression (1) by extrapolating to  $T = 0$ ,  $B_s(y) = 1$ , to determine  $g$ , and selecting  $T_c$  to give the best fit to the data at the higher temperatures. The values for the magnetic form factor are in each case taken from the form factor curve for  $Mn^{++}$  previously determined by Shull and Wollan. From the observed intensities of the first five magnetic reflections [(100), (001), (111), (210), (201)] it was found that the direction of spontaneous magnetization in  $MnF_2$  and  $FeF_2$  is along the  $c$  axis, hence  $q_{100}^2 = 1$ ; in the case of  $NiF_2$ , however, it appears that the ionic magnetic moments are aligned along one of the F-Ni-F directions so that  $q_{100}^2 = 0.80$ .

The  $g$  values of 1.99 and 2.02 for  $Mn^{++}$  and  $Ni^{++}$ , respectively, indicate that for these ions the scattering is due to electron spin only, whereas for  $Fe^{++}$  with  $g = 2.32$  there is presumably an additional scattering contribution due to the partially quenched orbital momentum of the electrons.

The 75°K curie temperature used for  $MnF_2$  agrees reasonably well with the temperature of maximum susceptibility (72°K) found by Bizette and Tsai,<sup>(9)</sup> and the temperature of zero anisotropy for the susceptibility of a single crystal (77°K) reported by Griffel and Stout.<sup>(10)</sup> For  $FeF_2$ , Bizette and Tsai<sup>(11)</sup> found a maximum susceptibility

(9) H. Bizette and B. Tsai, "Magnétisme. Susceptibilité magnétique à basse température du fluorure manganéux  $MnF_2$ ," *Compt. rend.* 209, 205 (1939).

(10) M. Griffel and J. W. Stout, "The Magnetic Anisotropy of Manganous Fluoride Between 12 and 295 K," *J. Chem. Phys.* 18, 1455 (1950).

(11) H. Bizette and B. Tsai, "Magnétisme. Le point de transition  $\lambda$  du fluorure ferreux  $F_2Fe$ ," *Compt. rend.* 212, 119 (1941).

at 79°K which seems much too small to fit the diffraction data of Fig. 3 with a Brillouin function of  $S$  only. These data, however, are probably inadequate to demonstrate a real difference between neutron diffraction and susceptibility measurements. The powder susceptibility of  $NiF_2$  has been measured by deHaas, Shultz, and Koolhaas<sup>(12)</sup> and Bizette,<sup>(13)</sup> and no evidence of antiferromagnetism was found.

Studies now in progress indicate that  $CoF_2$  becomes antiferromagnetic below about 40°K and has the same magnetic structure as  $MnF_2$ . Here again, as for  $NiF_2$ , the susceptibility as measured by Bizette<sup>(13)</sup> shows no antiferromagnetic behavior.

The present incomplete data on  $MnO_2$  show that this compound has an antiferromagnetic state below about 80°K, as is to be expected from the specific heat measurements of Millar<sup>(14)</sup> and the susceptibility measurements of Bizette.<sup>(15)</sup> The magnetic structure of  $MnO_2$  seems to be quite different from that of the fluorides; the exact nature of this difference is now being studied.

(12) W. J. deHaas, B. H. Schultz, and J. Koolhaas, "Further Measurements of the Magnetic Properties of Some Salts of the Iron Group at Low Temperatures," *Physica* 7, 57 (1940).

(13) H. Bizette, "Sur l'orientation par le champ magnétique de quelques molécules et de quelques cristaux," *Ann. Phys.* 1, p. 17, esp. p. 295 (1946).

(14) R. W. Millar, "The Specific Heats at Low Temperatures of Manganous Oxide, Manganous-Manganic Oxide and Manganese Dioxide," *J. Am. Chem. Soc.* 50, 1875 (1928).

(15) H. Bizette, Colloque sur les phénomènes cryomagnétiques (cerémonies Perrin-Langevin, 1948).

# UNCLASSIFIED

FOR PERIOD ENDING JUNE 20, 1951

## 2. SHORT-LIVED ISOMERS

F. K. McGowan

A promising line of investigation which has been extended by the development of scintillation detectors is the measurement of short-lived metastable states of nuclei. In order to detect a short-lived metastable state with half-lives less than  $10^{-4}$  sec advantage is taken of the fact that when they are produced as a consequence of a beta disintegration there is a time interval between the radiation announcing the formation of the state and the radiation emitted by the decay of the metastable state. For the measurement of the time intervals the method of delayed coincidences between two scintillation detectors is used.

A description of the apparatus used in a systematic search for the occurrence of excited nuclear states decaying with half-lives between  $5 \times 10^{-9}$  and  $10^{-4}$  sec, and the results of the survey have been previously reported.<sup>(1)</sup> An extension of the method to search for nuclear metastable states with lifetimes between  $10^{-10}$  and  $10^{-8}$  sec has been made possible through the use of Hewlett Packard 460A wide-band amplifiers, the scintillation spectrometer, and improved methods of analysis of delayed coincidence resolution curves.

Both the radiation announcing the formation of an excited state in  ${}^{160}_{66}\text{Dy}$  with a half-life  $(1.8 \pm 0.2) \times 10^{-9}$  sec and the radiation resulting from its decay have been studied with a delayed coincidence scintillation spectrometer using anthracene. The spectrum of the radiation announcing the formation of the metastable state

appears to be a  $\beta$ -ray distribution whose maximum energy is about .90 Mev, which is presumably the 860-Kev  $\beta$  ray observed in the decay of  $\text{Tb}^{160}$  from magnetic spectrometer measurements. The Land M internal conversion electrons corresponding to a 85-Kev transition are observed in the spectrum of the delayed radiation. No other  $\gamma$  rays appear in the spectrum of the delayed radiation. Using a NaI scintillation spectrometer  $\gamma$  rays were observed at the following energies: 85, 200, 296, 375, 875, and 960 Kev.

Under favorable conditions a half-life of  $5 \times 10^{-10}$  sec could be detected with the apparatus using anthracene. In many cases the lifetimes of the excited states are too short to be measured and only upper limits can be set. The observed upper limits on the half-life of excited states are listed in Table 3.

TABLE 3  
Nuclei Investigated for  
Short-Lived Isomers

NUCLEUS	$E_{\gamma}$ (Kev)	$T_{1/2}$ ( $10^{-9}$ sec)	RADIOACTIVE SOURCE
${}_{52}\text{Te}^{123}$	159	<1.0	$\text{Te}^{123}$ *
${}_{52}\text{Te}^{125}$	35	<2.0	$\text{Te}^{125}$ *
${}_{67}\text{Ho}^{165}$	95	<0.8	$\text{Dy}^{165}$
${}_{80}\text{Hg}^{198}$	411	<0.4	$\text{Au}^{198}$
${}_{81}\text{Tl}^{203}$	280	<0.4	$\text{Hg}^{203}$

(1) F. K. McGowan, *Short-Lived Isomeric States of Nuclei*, ORNL-952 (March 13, 1951).

# UNCLASSIFIED

## PHYSICS DIVISION QUARTERLY REPORT

Since a NaI scintillation detector employing a crystal 1.5 in. in diameter and 1 in. in length would have an intrinsic efficiency of 100% for  $\gamma$  rays with energies less than 150 Kev, it should be possible under favorable circumstances to measure K-shell internal conversion coefficients of  $\gamma$  rays by measuring the intensity of the K X-ray and the  $\gamma$  ray with a NaI scintillation spectrometer. Sources of uncertainty are the fluorescent yield of the K X-rays, the escape of the iodine K X-ray for incident X-ray energies slightly above 33 Kev (binding energy of K electrons in iodine), and K X-rays resulting from internal conversion of other  $\gamma$  rays other than the one of interest. Measurements of the

K-shell internal conversion coefficient for four  $\gamma$  rays in neighboring nuclei have been measured with a NaI scintillation spectrometer. A typical spectrum of the K X-ray and the 81-Kev  $\gamma$  ray following the beta decay of  $\text{Ho}^{166}$  is shown in Fig. 5. The pulse distribution has been resolved into three Gaussian components in Fig. 6. The peak at 20 Kev is the "escape" peak corresponding to the photoelectron energy produced by the K X-rays from the source incident on the detector with the escape of the iodine K X-ray. The peak at 49 Kev corresponds to the full energy of the K X-ray from the source being dissipated in the detector. The third peak at 81 Kev corresponds to

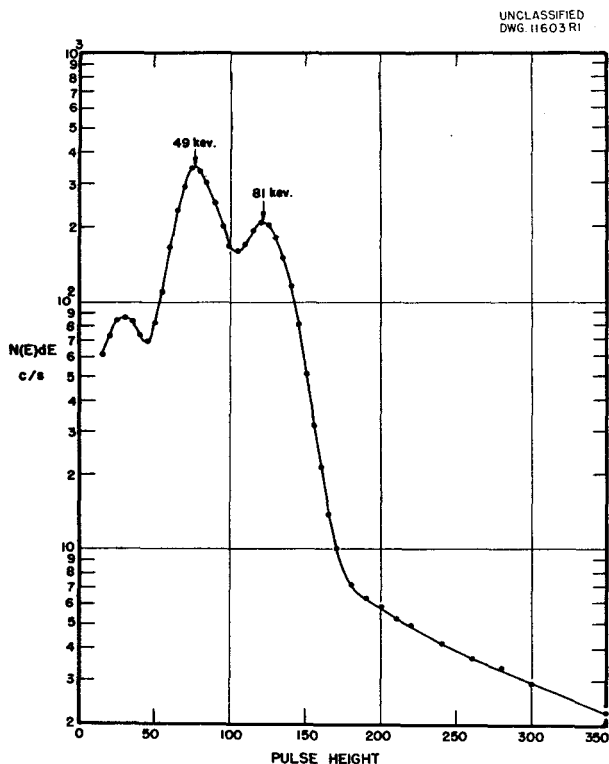


Fig. 5 - Low-Energy  $\gamma$ -Ray Spectrum from  $\text{Ho}^{166} \xrightarrow{\beta^-} \text{Er}^{166}$ .  
27 hr

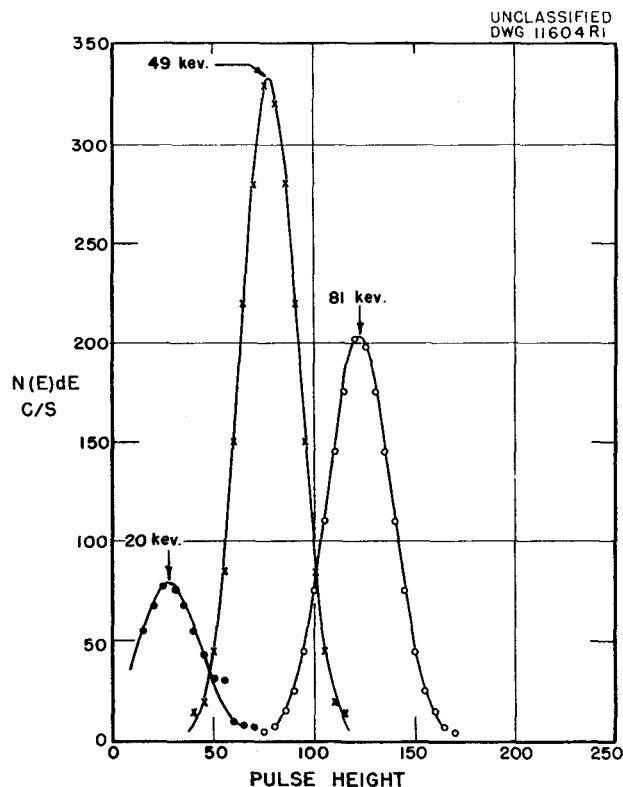


Fig. 6 - Low-Energy  $\gamma$ -Ray Spectrum from  $\text{Ho}^{166} \xrightarrow{\beta^-} \text{Er}^{166}$  Resolved into Gaussian Components.  
27 hr

# UNCLASSIFIED

FOR PERIOD ENDING JUNE 20, 1951

TABLE 4

Some Measured Internal Conversion Coefficients in the K-Shell

NUCLEUS	$E_\gamma$ (Kev)	$T_{1/2}$ ( $10^{-9}$ sec)	ENERGY OF K X-RAY (Kev)	INTENSITY OF ESCAPE PEAK (%)	FLUORESCENT YIELD, $\mathbb{W}_K^*$	K-SHELL INTERNAL CONVERSION COEFFICIENT, $\alpha_K = N_e/N_\gamma$
${}_{66}\text{Dy}^{160}$	85	1.8	46		.914	$\leq 2.4$
${}_{67}\text{Ho}^{165}$	95	<0.8	47.6	27	.918	$\leq 2.9$
${}_{68}\text{Er}^{166}$	81	1.7	49	26	.921	1.9
${}_{70}\text{Yb}^{170}$	85	1.6	52.5	24	.928	1.5

\*Semiempirical relation  $\mathbb{W}_K = \frac{Z^{3.5}}{Z^{3.5} + 2.2 \times 10^5}$ . See for instance, M. Haas, "Der Nutzeffekt der Rontgen-K-Fluoreszenzstrahlung bei leichten Elementen," *Ann. Physik* (5) 16, 473 (1933).

the full energy of the  $\gamma$  ray. The "escape" peak is about 26% of the full energy peak in intensity. The sum of areas under the 20-Kev and 49-Kev Gaussian components, after correcting for the fluorescent yield of the K X-rays, is then a measure of the number of K-shell internal conversion electrons. Likewise the area under the 81-Kev Gaussian component is a measure of the number of  $\gamma$  rays. The results of the measurements are tabulated in Table 4. Only the upper limit is indicated for  $\alpha_K$  in the cases of  $\text{Dy}^{160}$  and  $\text{Ho}^{165}$  because there are several other  $\gamma$  rays at higher energies which, if there is any internal conversion of these in the K-shell, will contribute

K X-rays to the observed intensity of the X-ray component in the measured spectrum. However, one may estimate an upper limit that these interfering  $\gamma$  rays may reduce the  $\alpha_K$  in Table 4 by using the upper limit of the lifetime of the higher energy transitions to fix the highest multipole order possible and the theoretical K-shell internal conversion coefficients.<sup>(2)</sup> The estimates indicate that  $\alpha_K$  could be reduced at the most by 30% and 20%, respectively. The latter two values of  $\alpha_K$  in Table 4

(2) M. E. Rose, G. H. Goertzel, and C. L. Perry, *K-Shell Internal Conversion Coefficients, Revised Tables*, ORNL-1023 (June 25, 1951).

# UNCLASSIFIED

## PHYSICS DIVISION QUARTERLY REPORT

are probably good to  $\pm 15\%$ . In the meantime it is necessary to wait until theoretical K-shell internal conversion coefficients become available for  $E_\gamma < 150$  Kev in order to fix the multipole order and character of the  $\gamma$ -ray transition. It is of interest to note that in the case of the 85-Kev tran-

sition of  $\text{Yb}^{170}$ , Elliott<sup>(3)</sup> measured the intensity of the K X-rays and  $\gamma$  rays with a proportional counter spectrometer and obtained  $\alpha_K = 1.8$ .

---

<sup>(3)</sup>L. G. Elliott, Montreal Report PR-P-7, p. 20 (Aug. 1950).

# UNCLASSIFIED

FOR PERIOD ENDING JUNE 20, 1951

## 3. INTERACTION OF LOW-ENERGY IONS WITH SOLIDS AND GASES

G. E. Evans      C. F. Barnett  
Paul Stier      V. L. DiRito  
J. W. Schwartz\*

The research of this section is primarily concerned with the phenomena associated with the passage of low-energy (approximately 20-Kev to 400-Kev) heavy positive ions through gases and solids. The specific phenomena of interest include single and multiple scattering in gases, capture and loss of electrons by ions, rate of energy loss and range of heavy ions in gases and solids, ionization produced in gases by passage of heavy ions, and effects of heavy-ion bombardment upon the properties of solid target materials. An ion source has been built which will permit the use of a wide variety of positive ions such as  $H^+$ ,  $He^+$ ,  $He^{++}$ ,  $A^+$ , etc. The major portion of the effort during the past quarter has been devoted to the design and construction of ion source assemblies, target assemblies, and associated instrumentation for use with the Cockcroft-Walton accelerator.

### ION SOURCE STUDIES

For some of the proposed experiments an ion source is needed which is compact, stable, high in ion output, and capable of producing positive ions of almost any atomic weight either from gaseous or solid source materials. A variety of PIG type sources have been built with these requirements in mind. In one type of ion source operated, ions are extracted perpendicularly to the magnetic field, and a positive probe placed in the plasma raises its

---

\*Summer research student.

potential for higher efficiency. In this ion source, total beam currents of about 1 ma are available at a power consumption in the source of 250 watts. This source operates stably only at pressures which are somewhat high for successful use in the Cockcroft-Walton accelerator. In a second type of ion source ions are extracted parallel to the magnetic field. This source has produced stable ion beams of 400  $\mu a$ , with a power consumption of 60 watts, and it appears likely that this output can be considerably increased by improved focussing. This axial source operates well at the pressure of the Cockcroft-Walton accelerator.

### DETECTION OF POSITIVE ION BEAM

A variety of methods for the detection and study of the positive ion beam are being investigated. An electron multiplier has been built and is being bench-tested. The response characteristics of the electron multiplier are to be studied as a function of mass and energy of the incident ions.

### GAS-SCATTERING APPARATUS

Since the range of low-energy heavy ions in solids is too small to permit the use of any type of window in the path of the beam, a windowless scattering chamber has been constructed. The positive ion beam enters the chamber through a system of three pin holes. Escape of gas from the scattering chamber into the accelerator is pre-

# UNCLASSIFIED

## PHYSICS DIVISION QUARTERLY REPORT

vented by the use of high-capacity vacuum pumps operating on the regions between pin holes. Escape of the beam from the scattering chamber for purposes of detection is effected by a similar differential pumping system. The gas scattering chamber is constructed from a large bellows, permitting the exit system of pin holes to be rotated relative to the entrance pin holes about an axis passing through the center of the scattering chamber. Since the pin hole systems act as effective collimators, the amount of beam scattered through any angle up to about  $60^\circ$  can be observed. By rotating the exit set of pin holes out of the way, the entrance pin hole system can be used alone. Equipment is now being built to permit measurement and control of gas pressure in the scattering chamber.

### BOMBARDMENT OF THIN SURFACE FILMS

It is planned to study the effect of heavy-ion bombardment upon solid targets. Since the range in solids of the heavy ions to be studied is quite small, the targets to be used consist of thin surface films evaporated onto the surface of a metal block whose

temperature can be controlled. As a preliminary experiment, the stability of gold targets evaporated onto aluminum is being studied. After preparation of the evaporated targets the gold is activated by exposure in the ORNL graphite reactor. Upon bombardment of these radioactive gold targets, the amount and angular distribution of the gold which spalls or sputters from the surface can be determined. By proper evaporation techniques it has been found possible to prevent spalling or flaking of gold from the surface during bombardment by 200-Kev protons, although sputtering of gold from the surface is always observed. The evaporation techniques and target assembly have been revised during the past quarter, and the work is continuing.

A cryostat for target cooling and temperature control within the range  $-195$  to  $+50^\circ\text{C}$  has been built, employing helium gas as a recirculating coolant. An ordinary 1/3-hp generator unit is being used as a helium recirculating pump and works quite effectively. Temperature control is achieved by passing part of the helium through a liquid nitrogen heat exchanger and recombining the hot and cold helium before passing through the target.

# UNCLASSIFIED

FOR PERIOD ENDING JUNE 20, 1951

## 4. HIGH VOLTAGE PROGRAM

### NEUTRON CROSS-SECTIONS

H. B. Willard	T. M. Hahn
J. K. Bair	E. D. Klema
F. P. Green	C. W. Snyder

**Thick Target ( $p, n$ ) Yields.** A High Voltage Corporation 5-Mv Van de Graaff generator has recently been acquired by the Laboratory. In order to adapt this machine to neutron studies, various preliminary experiments are in progress. Results obtained show that above 4.0 Mev the neutron background due to the machine itself (beam striking the analyzing chamber, extension tubes, and slits) increases rapidly with proton energy. Accordingly, various thick target ( $p, n$ ) yields have been measured to decide which materials were best suited for collimating the beam. These yields were measured with a Bonner type counter located on the beam axis directly in front of the target. The fast neutron response of this counter has yet to be measured, but it was designed to have a high sensitivity for threshold (10- to 100-Kev) neutrons. The results for tantalum, tungsten, molybdenum, and brass are shown in Fig. 7. As was expected, tantalum is the most satisfactory material available, and by using it to line the exit port of the analyzing chamber and for collimators in the extension tubes (leading to the target), the neutron background was reduced by a factor of nearly 100. The high backgrounds were presumably due to the  $\text{Cu}^{65}(p, n)$  and  $\text{Cu}^{63}(p, n)$  reactions resulting from the small amounts of copper in the aluminum of the chamber and extension tubes. The

slits in the analyzer are all made of tantalum and therefore give a minimum background.

**The  $\text{Be}^9(p, n)\text{B}^9$  Yield.** The neutron yield from protons on beryllium was measured as a function of energy, using a long counter placed 100 cm from the target and at  $0^\circ$  to the beam. The energy range studied was from the threshold at  $2.059 \pm .002$  Mev<sup>(1)</sup> up to 5.1 Mev. The result shown in Fig. 8 gives the "geometric" peak indicating a target thickness of less than 10 Kev, a resonance at 2.58 Mev previously observed by Hushley,<sup>(2)</sup> and a new resonance at about 4.5 Mev, both resonances being in  $\text{B}^{10}$ , the compound nucleus.

**5-Mv Machine Calibration and Performance.** The installation of the 5-Mv electrostatic accelerator was completed on April 10. Considerable time and effort were expended in adjusting the machine for proper operation, and the final acceptance tests were run on May 9. Using the most recent generating voltmeter calibration of energy [neutron threshold measurements:  $\text{Li}^7(p, n)\text{Be}^7$  monatomic beam, 1.882 Mev;  $\text{B}^{11}(p, n)\text{C}^{11}$  monatomic beam, 3.015 Mev;  $\text{Li}^7(p, n)\text{Be}^7$  diatomic beam, 3.764 Mev], it appears that reliable performance may be obtained up to 5.5 Mv, with a maximum performance of 6.0 Mv. The analyzed proton beam measures from 1 to 4  $\mu\text{a}$  with a resolution of 0.1 percent. Stability below 1.5 Mv is not yet satisfactory, which, however,

(1) H. T. Richards and R. V. Smith, "P-N Thresholds for Calibration Points on the Nuclear High Voltage Scale," *Phys. Rev.* 77, 752 (1950).

(2) W. J. Hushley, "Gamma-Rays from Beryllium Caused by Proton Bombardment," *Phys. Rev.* 67, 34 (1945).

UNCLASSIFIED

# UNCLASSIFIED

## PHYSICS DIVISION QUARTERLY REPORT

UNCLASSIFIED  
DWG. 11738R1

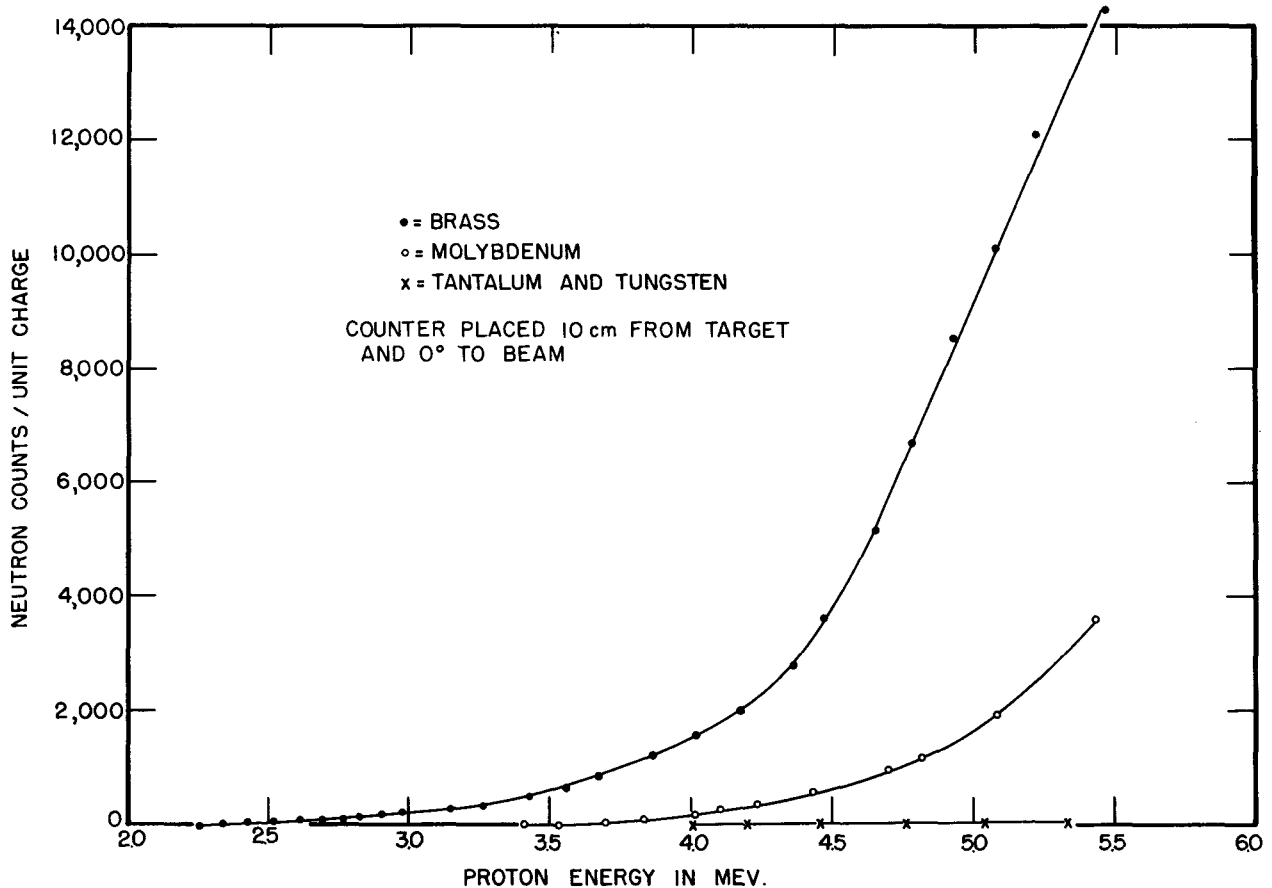


Fig. 7 - Thick Target ( $p, n$ ) Yield Curves Measured with Bonner Type Counter.

does not seem to be too important. The corona control regulator has been altered to operate from the mass one slits, hence the mass two beam may be brought up to the target by the magnet, giving acceptable operation down to 0.75 Mv.

### GAMMA-RAY SPECTROSCOPY

**Capture Gamma Rays from Protons on  $N^{14}$**  (C. H. Johnson, C. D. Moak, and G. P. Robinson). The  $\gamma$ -ray spectrum

has been observed for the resonant capture of protons by nitrogen. Protons from the Cockcroft-Walton generator were used to bombard a thick water-cooled TaN target prepared by heating tantalum in a nitrogen atmosphere. Capture  $\gamma$  rays were detected with a NaI(Th) crystal 2 in. in length and 1.5 in. in diameter placed to subtend a large solid angle at 0° to the proton beam. Scintillations produced in the crystal were detected by a type 5819 photomultiplier. Pulses from the

# UNCLASSIFIED

FOR PERIOD ENDING JUNE 20, 1951

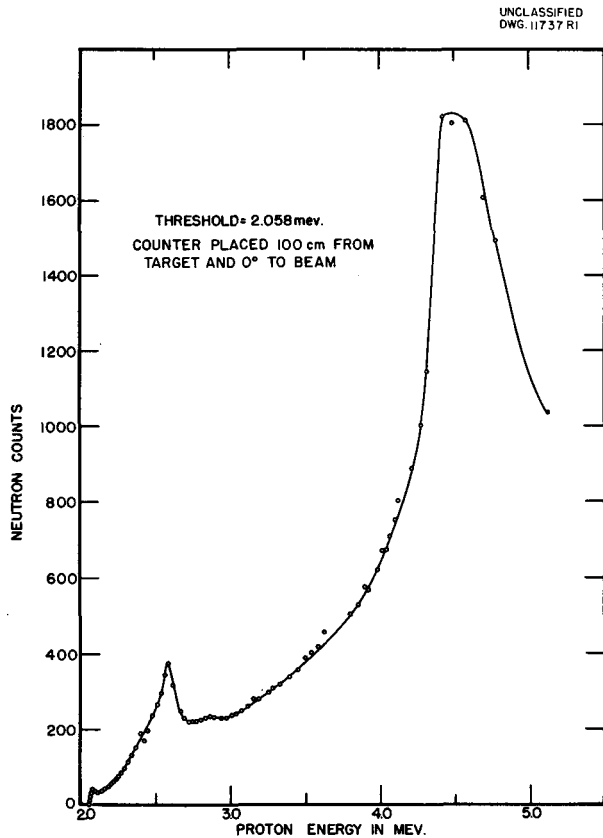


Fig. 8 -  $\text{Be}^9(p,n)\text{B}^9$  Yield Curve Measured with Long Counter.

photomultiplier were amplified with a linear amplifier and studied with a single channel differential analyzer.

The thick target yield curve showed a sharp rise near 277 Kev in agreement with the  $\text{N}^{14}(p,\gamma)$  resonance observed by Tangen.<sup>(3)</sup> The proton energy was set 10 Kev beyond this resonance and the  $\gamma$ -ray pulse height spectrum shown in the lower part of Fig. 9 was obtained. Figure 9 shows the differential counts per integral count received by the analyzer as a function of the pulse height accepted by the differential

(3) R. Tangen, *K. Norske videnskabers selskab*, BdXV, Nr 46.

channel. Integral bias settings were well above background. Pulse heights have been converted to energy by comparison with the photoelectric peaks produced by the  $\text{Cs}^{137}$  (0.66 Mev) and  $\text{Na}^{22}$  (1.277 Mev)  $\gamma$  rays. Calibrations with these sources were made at regular intervals to check the gain of the system.

To aid in the interpretation of this spectrum the pulse height distributions of the  $\text{Na}^{22}$  (1.277 Mev) and  $\text{Na}^{24}$  (2.75 Mev)  $\gamma$  rays and of the capture  $\gamma$  rays of protons on deuterium<sup>(4)</sup> are shown in the upper part of Fig. 9. In the energy region below 2 or 3 Mev  $\gamma$  rays show pronounced photoelectric peaks of pulse height corresponding to the  $\gamma$ -ray energy. The presence of a Compton peak of slightly lower pulse amplitude may aid in the identification of such groups; thus the groups found at B and C in Fig. 9 are photoelectric peaks. In the higher energy region only pair production yields a pronounced peak at a pulse amplitude 1.02 Mev less than the  $\gamma$ -ray energy. Pair peaks observed with a large crystal show a "fine structure" since one or both of the annihilation quanta may be captured within the crystal to give rise to small peaks 0.51 and 1.02 Mev above the main pair group. The capture  $\gamma$  rays of protons on deuterium show some of this structure even though that data was taken with somewhat poorer resolution than was used in the present measurements. Since the groups at A' and B' are separated by more than 0.51 Mev, the peak at A' cannot be attributed to fine structure; however, the group about 0.5 Mev above A' may result from this structure. These

(4) G. Robinson, C. D. Moak, and W. M. Good, "High-Voltage Program. Scintillation-Counter Gamma-Ray Spectra," *Physics Division Quarterly Progress Report for Period Ending March 20, 1951*, ORNL-1005, p. 26 (July 24, 1951).

UNCLASSIFIED

# UNCLASSIFIED

## PHYSICS DIVISION QUARTERLY REPORT

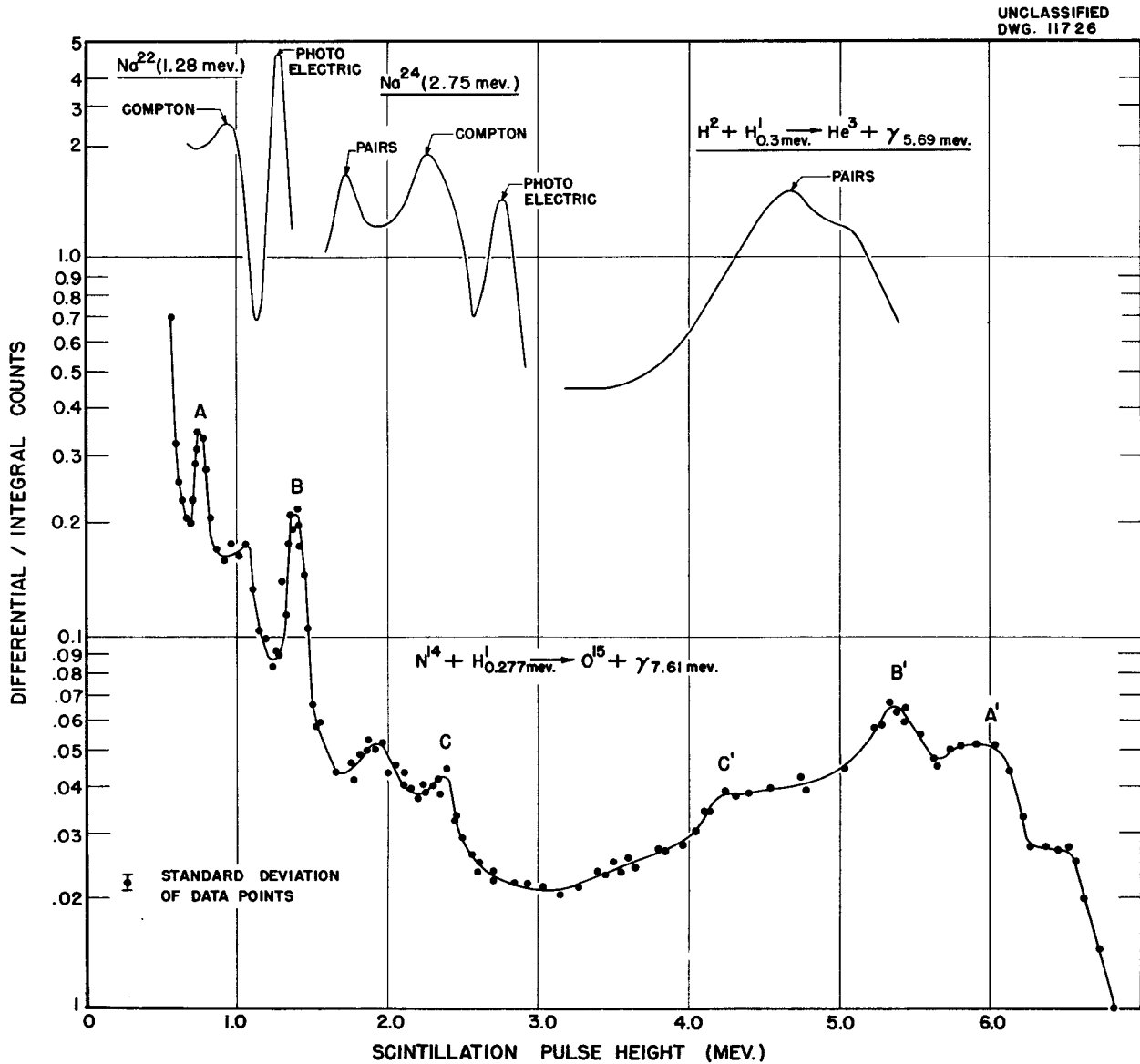


Fig. 9 - Gamma Rays from  $N^{14}(p,\gamma)$  Reaction.

considerations indicate photoelectric peaks at A, B, and C and pair production peaks at A', B', and C' (Fig. 9).

The only reaction energetically possible for 277-Kev protons on  $N^{14}$  is proton capture followed by positron

# UNCLASSIFIED

FOR PERIOD ENDING JUNE 20, 1951

decay to  $N^{15}$ . Positron decay could leave  $N^{15}$  with up to 1.68 Mev excitation; however, since the observed positron spectrum is not complex,<sup>(5)</sup> it is assumed the decay occurs to the ground state and all  $\gamma$  rays result from the direct capture process. According to recent mass values<sup>(6)</sup> 277-Kev protons on  $N^{14}$  form  $O^{15}$  with 7.61-Mev excitation. The six  $\gamma$  rays found from Fig. 9 can be arranged to give the total excitation energy only if there are three intermediate levels in  $O^{15}$  giving rise to three cascade processes of two  $\gamma$  rays each. The following additions of the energies (including in each case the 1.02 Mev needed for pair production) show that the groups add to give the total excitation:

$$A + A' = 0.75 + (6.00 + 1.02) = 7.77 \text{ Mev}$$

$$B + B' = 1.38 + (5.35 + 1.02) = 7.75 \text{ Mev}$$

$$C + C' = 2.38 + (4.25 + 1.02) = 7.65 \text{ Mev}$$

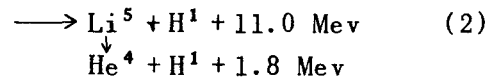
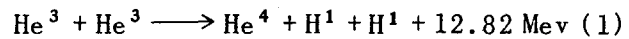
In each addition the discrepancy from the 7.61-Mev excitation is considered within experimental error. A crossover transition yielding a 7.61-Mev  $\gamma$  ray was not detected.

## CHARGED PARTICLE REACTIONS

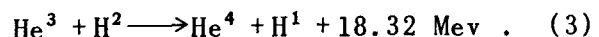
**The Reaction of  $He^3 + He^3$**  (W. M. Good, W. E. Kunz, and C. D. Moak). Provision has been made on the Cockcroft-Walton generator for the acceleration of  $He^3$  and  $H^3$ . The equipment consists of special gas metering equipment in the high-voltage terminal to maintain constant pressure in the ion source, together with automatic Toepler

pumping to back up the diffusion pumps and conserve the gas.

With a mixture of 2.5%  $He^3$  and 97.5%  $He^4$  being fed into the ion source, a 3- $\mu$ a beam of magnetically separated  $He^{3+}$  can be obtained. Reactions involving the capture of  $He^3$  by  $He^3$ , which have so far not been reported, have been observed. The reactions expected are the following:



The results, which are preliminary, were obtained as follows: The beam of separated  $He^{3+}$  at 300 Kev was made to fall upon a 5-mil aluminum foil at the end of the tube down which the  $He^{3+}$  beam passed. Behind the foil corresponding to reaction products at  $0^\circ$  to the beam was placed the proton detector. At a short time after allowing the beam of  $He^3$  to strike the aluminum foil there appeared protons which were identified as the 14.68-Mev protons from the reaction



The reason for the appearance of this reaction is the presence of deuterium in the system subsequent to its use in the accelerator. In addition to these protons, there appeared a counting rate which varied with time and which rose to a limiting value in the course of about 2 hr. On the assumption that these counts were caused by protons, the spectrum was obtained by two methods using a fresh target of clean 5-mil aluminum foil each time. The first of these methods consisted of biasing a proportional counter to correspond to a proton at

(5) H. Brown and V. Perez-Mendez, "Beta-Spectra of Gaseous  $A^{41}$  and  $O^{15}$ ," *Phys. Rev.* 78, 649 (1950).

(6) Li, W., Whaling, W. A. Fowler, and C. C. Lauritzen, private communication.

UNCLASSIFIED

# UNCLASSIFIED

## PHYSICS DIVISION QUARTERLY REPORT

the end of its range. The counting rate of this counter was then taken for different thicknesses of aluminum absorber between the target and the counter. The resulting curve is shown in Fig. 10, in which the range, including that of the 5-mil aluminum target, has been converted to energy. The 14.68-Mev protons from the impurity reaction (3) have the correct range within experimental error. The second

method consisted of observing the spectrum of pulses produced in a thin NaI crystal and a 5819 photomultiplier by these protons. In this case the 14.68-Mev protons from (3) were used to give the energy calibration of the spectrometer, account being taken again of the loss of energy in the 5 mils of the target that the protons had to traverse. The spectrum obtained by this method is also shown in Fig. 10.

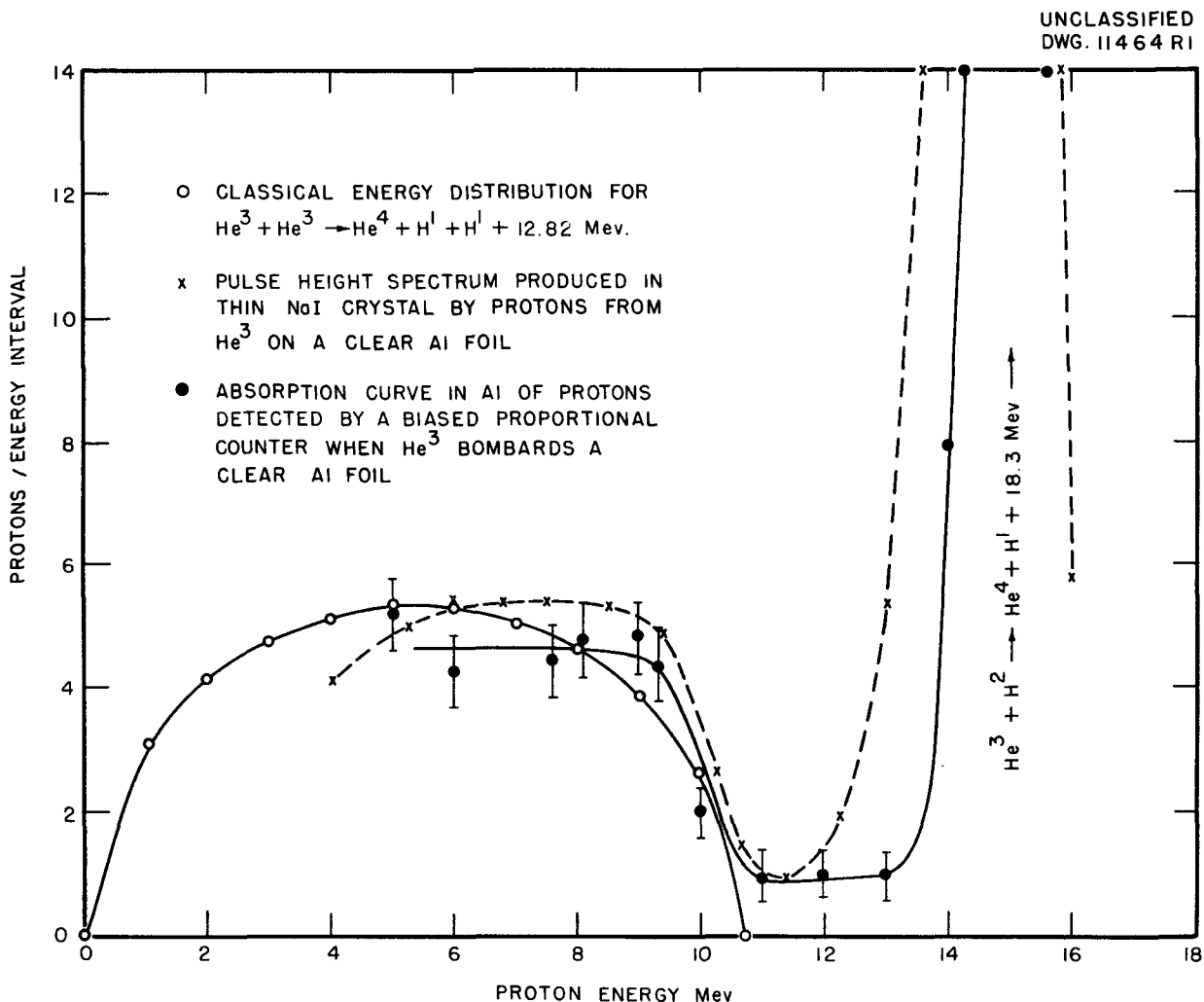


Fig. 10 - Energy Distribution of Protons from Bombarding  $\text{He}^3$  on Clean Aluminum.

# UNCLASSIFIED

FOR PERIOD ENDING JUNE 20, 1951

In order to identify the reaction taking place Fig. 10 also gives the statistical proton energy distribution corresponding to reaction (1). The maximum energy of the observed distribution agrees within the errors of the experiment with the maximum energy of

the spectrum corresponding to (1). Since the protons of reaction (2) are less energetic than those from reaction (1), at least some of mode (1) is present. This reaction is being studied further for evidence which it might yield on levels in  $\text{Li}^5$ .

UNCLASSIFIED

# UNCLASSIFIED

## PHYSICS DIVISION QUARTERLY REPORT

### 5. SHORT-PERIOD ACTIVITIES

E. C. Campbell      J. H. Kahn  
K. L. Robertson

By means of a special pneumatic tube installed in the Oak Ridge graphite reactor it is possible to irradiate samples inside the reactor and then eject them very quickly into a shielded counter or spectrometer where the decay can be followed and automatically recorded. In this way several new radioactive species have been discovered having half-lives in the region between 0.3 sec and several seconds. The scintillation and proportional counter spectrometer with photographic recording of self-triggered pulses on a cathode-ray oscillograph provides a means for studying the radiation emitted by these substances. Recently a program has been undertaken to investigate the X rays associated with radioactive decay and to determine by these measurements the coefficients of internal conversion.

#### DOUBLE-CHANNEL COINCIDENCE SPECTROMETER

E. C. Campbell

If the decay of a radioactive substance is complex it is not usually possible to disentangle the various emitted radiations and to construct a unique decay scheme without the use of the method of coincidences. With scintillation detectors it would be ideally desirable to employ two multichannel pulse analyzers in order to ascertain the pulse height of each of two coincident pulses. The conventional multichannel analyzer is an exceedingly complicated instrument; to build two of them for this purpose seems impractical.

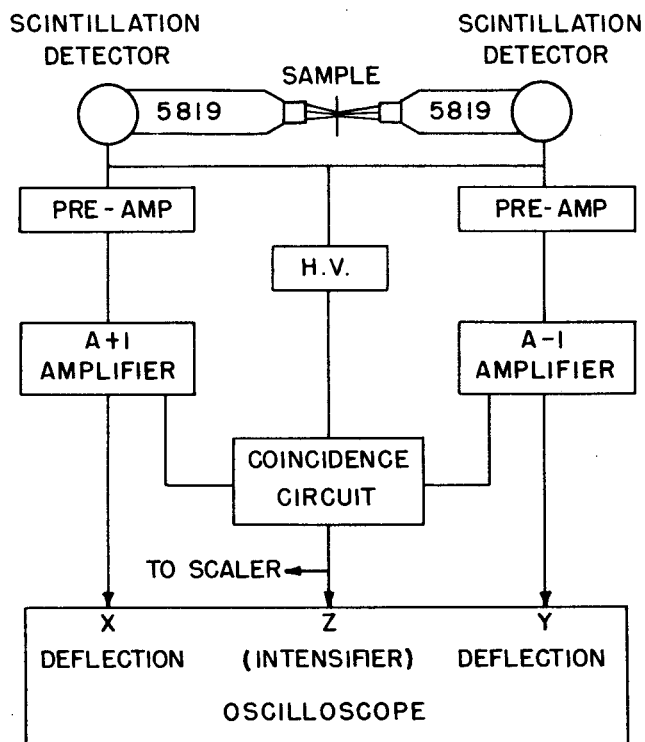
A relatively simple method has been devised as an adaptation of the photographic method of pulse analysis which accomplishes the desired objective and is particularly well adapted to studies of short-period radioisotopes. In Fig. 11a is shown a block diagram of the apparatus as now used.

Two separate scintillation detectors [NaI(Tl) or anthracene] are used, each provided with its own A-1 amplifier. The pulse output of one amplifier is connected to the horizontal deflection amplifier of a Dumont 248-A cathode-ray oscilloscope; that of the other is connected to the vertical deflection amplifier. The constant amplitude pulses from the separate pulse height selector output of the A-1 amplifiers are fed to a coincidence circuit which has a resolving time of about 0.5  $\mu$ sec, designed by Dr. J. D. Palmer of the Instrument Department. The output of the coincidence circuit then is connected to the z-axis amplifier of the oscilloscope, which, in effect, turns on the beam only when coincident pulses are received. The triple of pulses is shown in Fig. 11b. What appears on the screen of the oscilloscope, then, in the ideal case, is a succession of bright spots (only one shown in Fig. 11c), the coordinates of which give separately the pulse heights of the two coincident pulses, one in each of the two channels. These can be photographed, and the coincidence spectrum can be interpreted once the energy calibration has been made for each detector channel. Actually it is somewhat difficult to adjust the phase

# UNCLASSIFIED

FOR PERIOD ENDING JUNE 20, 1951

UNCLASSIFIED  
DWG. 11670



(a)

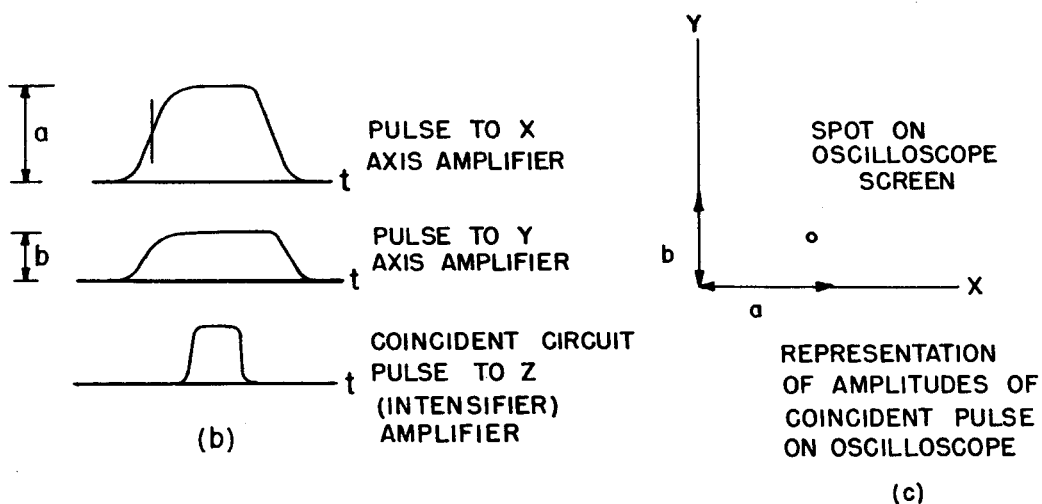


Fig. 11 - Double Channel Coincidence Spectrometer.

# UNCLASSIFIED

# UNCLASSIFIED

## PHYSICS DIVISION QUARTERLY REPORT

of the pulses so that the intensifier pulse occurs at the peak of both the  $x$  and  $y$  pulses. The result is that one sees on the oscilloscope short line segments instead of a bright spot as desired.

This defect can be remedied, according to a suggestion of P. R. Bell, by suitable pulse-lengthening circuits which operate only on the coincident pulses. Such a circuit is now being designed for this purpose by G. G. Kelley.

In the case that it is desired to look at the whole coincident pulse spectrum in either channel, the most convenient method is to use the pulse output of the coincidence circuit to trigger the horizontal sweep of the oscilloscope while the pulse output of one channel is connected to the  $y$ -axis deflection amplifier through a delay line.

After the present apparatus had been set up and tested, an abstract<sup>(1)</sup> by R. F. Post was received in which a similar scheme of coincident pulse

analysis is proposed for use in a pair spectrometer. In his method no separate coincidence circuit is used; every pulse in the  $x$ -channel intensifies the beam. This method has the disadvantage that all of the many noncoincident pulses are displayed as a bright trace along the  $x$ -axis. The extra scattered light would be undesirable if the coincident pulses are to be photographed. The oscilloscope method is a slight extension of a technique developed by H. Kallman and C. A. Accardo,<sup>(2)</sup> who have obtained triple coincidences from three photomultipliers, each detecting light flashes in the same phosphor. The three photomultipliers were connected one to each of the  $x$ ,  $y$ , and  $z$  axis amplifiers of the oscilloscope. In this way they were able to reduce the number of random noise pulses very considerably. Mention is also made of the possibility of using this method to reduce noise with two separate detectors, but the utility of the method for coincident pulse analysis is not pointed out.

---

<sup>(1)</sup>*Bull. Am. Phys. Soc.* 26, 6 (1951).

---

<sup>(2)</sup>H. Kallmann and C. A. Accardo, "Coincidence Experiments for Noise Reduction in Scintillation Counting," *Rev. Sci. Instruments* 21, 48 (1950).

# UNCLASSIFIED

FOR PERIOD ENDING JUNE 20, 1951

## 6. HARD GAMMA EMITTERS AMONG FISSION FRAGMENTS<sup>(1)</sup>

W. K. Ergen

A compilation of fission fragments with half lives longer than ~3 hr and with known or suspected gamma energies above the Be( $\gamma, n$ ) threshold in their own or in their daughters spectrum is presented in Table 5. These gammas cause photoneutron emission in deuterium and beryllium, and the superposition of activities with the half lives of Table 5 fit the measured<sup>(2,3)</sup> photoneutron activities caused by the neutron irradiated U<sup>235</sup> in deuterium

and beryllium. The fit is good to about 5% at waiting times greater than about 10 hr. In order to obtain this fit one has to postulate certain intensities for the gammas in the spectra of the individual fission fragments, and these postulated intensities agree remarkably well with the intensities measured by independent means, with but few exceptions. These are discussed in more detail in ANP-59.<sup>(1)</sup>

TABLE 5

Hard Gamma Emitters Among Fission Fragments

NUCLIDES	HALF-LIFE <sup>(4)</sup>	YIELD, <sup>(5)</sup> y (%)	FRACTION OF TRANSITIONS PRODUCING HARD GAMMAS, f (%)	GAMMA ENERGY, E (Mev)	BERYLLIUM PHOTONEUTRON CROSS-SECTION, $\sigma_{Be}$ (mb)	DEUTERIUM PHOTONEUTRON CROSS-SECTION, $\sigma_D$ (mb)	$yf\sigma_{Be}$ ( $10^4$ mb)		$yf\sigma_D$ ( $10^4$ mb)	
							CALC.	EXP.	CALC.	EXP.
Ru <sup>106</sup> ; Rh <sup>106</sup>	1 year; 30 sec	0.48	2	2.9 <sup>(6)</sup>	0.85	1.79	0.82		1.7	
Ce <sup>144</sup> ; Pr <sup>144</sup>	275 days; 17.5 min	5.3	weak 2 2	>2.2 <sup>(6)</sup> 2.185 <sup>(6)</sup> 2.6 <sup>(7)</sup>	0.53 0.48	1.36	5.6		14.4	
Eu <sup>156</sup>	15.4 days	0.013	60	2 <sup>(8)</sup>	0.6		0.47		0	0
Ba <sup>140</sup> ; La <sup>140</sup>	12.8 days; 40 hr	6.1	3.2	2.5 <sup>(9)</sup>	0.36	1.19	7.07	6.8	23.2	23.2
Te <sup>132</sup> ; I <sup>132</sup>	77.7 hr; <sup>(10)</sup> 2.4 hr	4.5 <sup>(10)</sup>	2.7	2.0 <sup>(11)</sup>	0.6		7.3	7.2	0	0
Te <sup>131*</sup> ; Te <sup>131</sup>	30 hr; 25 min	0.45 <sup>(10)</sup>	21.6	>2.2 <sup>(12)</sup>	0.36	1.19		3.5		11.6
I <sup>135</sup>	6.7 hr	5.6	1.95 4	2.4 <sup>(13)</sup> 1.8 <sup>(14)</sup>	0.23 0.8	1.03	17.9	198	11	11.0
Kr <sup>88</sup> ; Rb <sup>88</sup>	2.77 hr; 17.8 min	3.1 <sup>(+)</sup>	<15 19 - 34	2.8 <sup>(15)</sup> 1.85 <sup>(15)</sup>	0.73 0.73	1.65	43 - 77	~0	<77	136

(+) Interpolated.

(1) Abstracted from the following report: W. K. Ergen, *Hard Gamma Emitters Among Fission Fragments*, ANP-59 (May 3, 1951).

(2) S. Bernstein, W. M. Preston, G. Wolfe, and R. E. Slattery, "Yield of Photo-Neutrons from U<sup>235</sup> Fission Products in Heavy Water," *Phys. Rev.* 71, 573 (1947).

(3) S. Bernstein, F. L. Talbott, J. K. Leslie, and C. P. Stanford, *Yield of Photoneutrons from U<sup>235</sup> Fission Products in Be*, CNL-38 (Feb. 20, 1948).

(4-15) Footnotes 4 through 15 appear on the following page.

# UNCLASSIFIED

## PHYSICS DIVISION QUARTERLY REPORT

(4) K. Way, L. Fano, M. R. Scott, and K. Thew, *Nuclear Data*, Nat. Bur. Standards (U.S.) Circular 499 (Sept. 1, 1950).

(5) K. Way and N. Dismuke, *Fission Product Yields*, ORNL-280, pp. 23-25 (Aug. 29, 1949).

(6) D. E. Alburger, E. der Mateosian, M. Goldhaber, and S. Katcoff, "Gamma Rays in the Decay of  $Rh^{106}$  and  $Pr^{141}$ ," *Phys. Rev.* 82, 332 (1951).

(7) C. E. Mandeville and E. Shapiro, "Radiations from Cerium (144)  $\beta$ , Praseodymium (144)  $\beta$ , Neodymium (144)," *Phys. Rev.* 79, 243 (1950).

(8) L. Winsberg, "Study of the Fission Chain  $10h Sm^{(156)} - 15.4d Eu^{(156)}$ ," paper 198 in *Radiochemical Studies: The Fission Products*, Ed. by C. D. Coryell and N. Sugarman, p. 1302, McGraw-Hill, New York, 1951.

(9) B. Russell, D. Sachs, A. Wattenberg, and R. Fields, "Yields of Neutrons from Photo-Neutron Sources," *Phys. Rev.* 73, 545 (1948).

(10) A. C. Pappas and C. D. Coryell, "Activities and Fission Yields in Chains of Masses 129 to 134," *Phys. Rev.* 81, 329 (1951).

(11) F. C. Maienschein, J. K. Bair, and W. B. Baker, "Gamma-Radiation from  $I^{132}$ ," *Phys. Rev.* 83, 477 (1951); G. W. Parker, private communication.

(12) G. W. Parker to W. K. Ergen, private communication.

(13) H. A. Levy and M. H. Feldman, ORNL-286, p. 80 (Sept. 14, 1949).

(14) A. D. Bogard *et al.*, ORNL-65, p. 59 (July 9, 1948).

(15) M. E. Bunker, L. M. Langer, R. J. D. Moffat, "The Disintegration of  $Rb^{88}$ ," *Phys. Rev.* 81, 30 (1951).

# UNCLASSIFIED

FOR PERIOD ENDING JUNE 20, 1951

## 7. TIME-OF-FLIGHT SPECTROMETER

G. S. Pawlicki and E. C. Smith

A time-of-flight neutron spectrometer for the measurement of total neutron cross-sections at energies up to 5000 ev is now under construction. Located at the face of the reactor will be a rotating shutter which cuts a neutron beam into bursts of small duration. Pulses from a detector 10 meters from the chopper are fed to an 84-channel chain-gated counting circuit which sorts the pulses according to the time the neutrons spend in transit.

The counting channels have been completed, and installation in the reactor building is in progress. Tests

show that they are performing according to design specifications.

The detector is an electron pulse ionization chamber with a sensitive volume 4 in. high, 6 in. wide and 12 in. long. It has been tested with un-enriched boron trifluoride. A study of methods of purification of  $\text{BF}_3$  and measurements of the drift velocities of electrons in that gas have been made. The chamber is being filled with 1 atm of enriched  $\text{BF}_3$ .

The rotating shutter is still under construction.

UNCLASSIFIED

# UNCLASSIFIED

## PHYSICS DIVISION QUARTERLY REPORT

### 8. INVESTIGATIONS WITH THE SCINTILLATION SPECTROMETER

#### $I^{131}$ GAMMA RAYS

P. R. Bell      J. E. Francis  
R. C. Davis     Judith Cassidy

Since the previous coincidence spectrometer measurements of  $I^{131}$ , the resolution of the spectrometer has been much improved. The  $\gamma$  rays have been run with the new resolution and another  $\gamma$  ray not found previously has been detected. This  $\gamma$  ray of approximately 0.5 Mev energy does not fit the previous decay scheme. In addition, the re-examination of the coincidence spectrometer information shows entirely too few coincidences per  $\gamma$  ray for the 638-Kev—80-Kev coincidences. Further, a search by the Chemistry Division group for coincidences between the 638-Kev  $\gamma$  ray and conversion electrons from the 80-Kev  $\gamma$  ray showed no coincidences. The error was due to the appearance of a random sum line when the 284-Kev and 364-Kev radiations were detected simultaneously, giving a peak at 644 Kev, coincident with 80 Kev because the 284-Kev radiation was involved. Correction for random pulses does not, of course, remove this. No 80-638 coincidences are found, and the two Kurie plots in the previous quarterly must be interpreted as two  $\beta$  rays of 255 and 335 Kev, coincident with the 724- and 638-Kev  $\gamma$  rays, respectively.

Figure 12 shows the curve obtained with  $I^{131}$ . The resolution of the 284-Kev  $\gamma$  ray and the 720-Kev  $\gamma$  ray is also considerably better, and these radiations can be seen easily now. The energies marked on the curve are the accepted energies of the main radiations

and not those obtained by calibration, although the agreement is good.

Further work on the coincidence spectrometer with the improved resolution is now in progress.

#### HOLLOW-CRYSTAL SPECTROMETER

P. R. Bell      J. E. Francis  
R. C. Davis     Judith Cassidy

Work with the hollow-crystal spectrometer, reported in a previous quarterly report<sup>(1)</sup> has been continued, and very good results have been obtained. Figure 13 shows a diagram of the arrangement showing the source, the collimator, and the hollow crystal itself mounted on the photomultiplier. Electrons entering the hole in the crystal are not readily scattered out since the solid angle of the hole is small at the place where the electrons strike. The layer of air between the crystal and the source causes considerable difficulty both absorbing and scattering soft electrons and spoiling the resolution.

Figure 14 shows some curves obtained using a  $Ca^{45}$   $\beta$ -ray source and various conditions of the apparatus. The lower curve shows the results obtained with air at atmospheric pressure between the crystal and source. Without moving the source, hydrogen was introduced into

---

(1)P. R. Bell, J. M. Cassidy, R. C. Davis, and G. G. Kelley, "Investigations with the Scintillation Spectrometer. Hollow-Crystal Spectrometer," *Physics Division Quarterly Progress Report for Period Ending December 20, 1950*, ORNL-940, p. 36 (March 15, 1951).

# UNCLASSIFIED

FOR PERIOD ENDING JUNE 20, 1951

UNCLASSIFIED  
DWG. 11722 RI

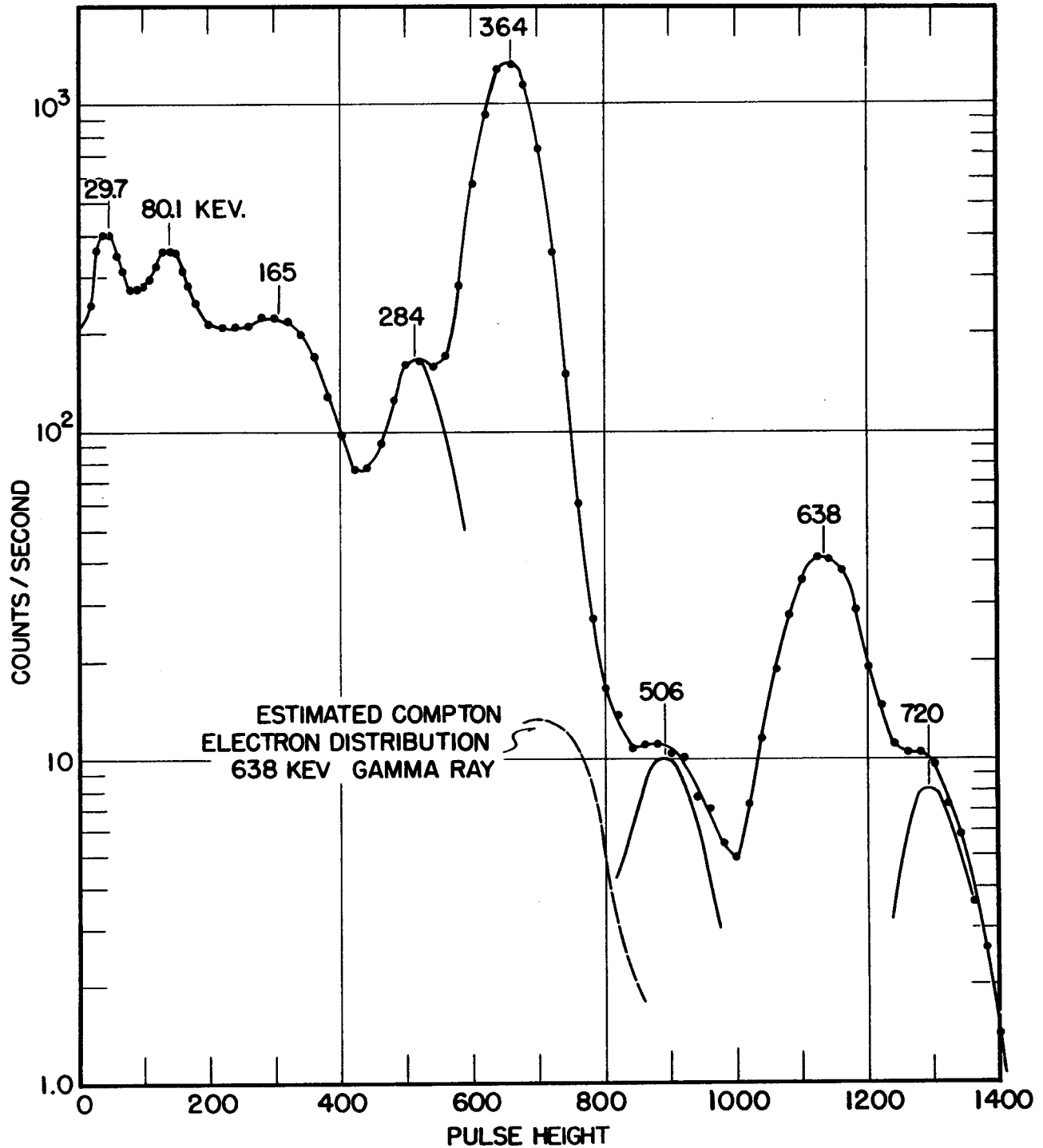


Fig. 12 -  $I^{131}$   $\gamma$  Rays Using NaI Crystal (5/23/51).

# UNCLASSIFIED

# UNCLASSIFIED

## PHYSICS DIVISION QUARTERLY REPORT

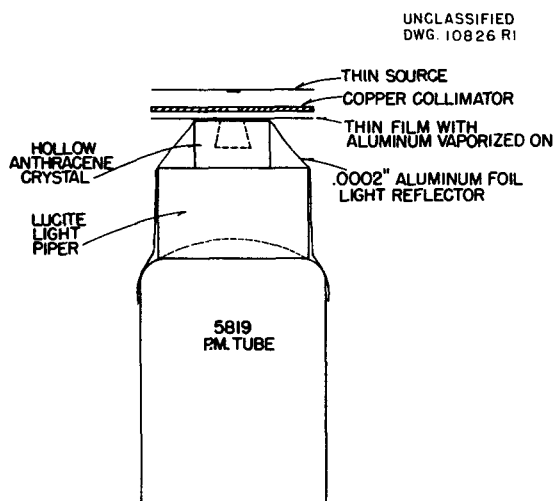


Fig. 13 - Hollow Crystal Spectrometer.

the container and resulted in the intermediate curve. Very many more electrons, even of considerable energy, are apparent. The container holding the crystal and the source was then evacuated and the upper curve obtained. As you can see, it was only slightly different, and so hydrogen is customarily used now in preference to vacuum, as handling the apparatus under these conditions is much easier.

Figure 15 is a Kurie plot obtained with this instrument for the radiations of  $\text{Ca}^{45}$ . A good Kurie plot was obtained and the end point at 245 Kev agrees with the work of Ketelle. The deviation below the line at 50 Kev is still partially unexplained. Part of the deviation is caused by the  $1/10 \text{ mg/cm}^2$  aluminum reflector window over the crystal, and part of it is probably due to the uncertainty in the curvature of the pulse height vs. energy curve for

anthracene. A correction has been applied to the data for this curvature according to the work of Hopkins, but the data is insufficient to get an accurate correction and further work must be done to get good corrections in the low-energy region. With proper correction curves there seems to be no reason why Kurie plots could not be obtained which are straight down to the order of 10 Kev at least.

The hollow-crystal spectrometer is now being used for studying the  $\beta$ - $\gamma$  coincidence spectra from  $\text{I}^{131}$ .

### IMPROVEMENT OF RESOLUTION OF SCINTILLATION SPECTROMETERS

P. R. Bell            J. E. Francis  
R. C. Davis         Judith Cassidy

In an effort to improve the resolution of the scintillation spectrometer, the optical absorption of the materials used in the spectrometer has been studied at some length. A Beckman Model DU quartz spectrophotometer was used for measuring the absorption of samples of anthracene, sodium iodide, mineral oil, and Canada balsam. The absorption spectra are shown in Fig. 16. It is interesting to notice that the anthracene absorption is extremely sharp and sets in abruptly at 4450 A and is essentially complete at 4250 A. The absorption of sodium iodide, however, shows a distinct step in the absorption, being only partially absorbing from 3250 to 3450 A. This sample, nearly 1 cm thick, would show poor resolution for any light emitted in the partially absorbed region since then the pulse would vary in size depending upon where in the crystal the similar light flashes were produced. The data for Canada balsam show a

# UNCLASSIFIED

FOR PERIOD ENDING JUNE 20, 1951

UNCLASSIFIED  
DWG. 10824 R1

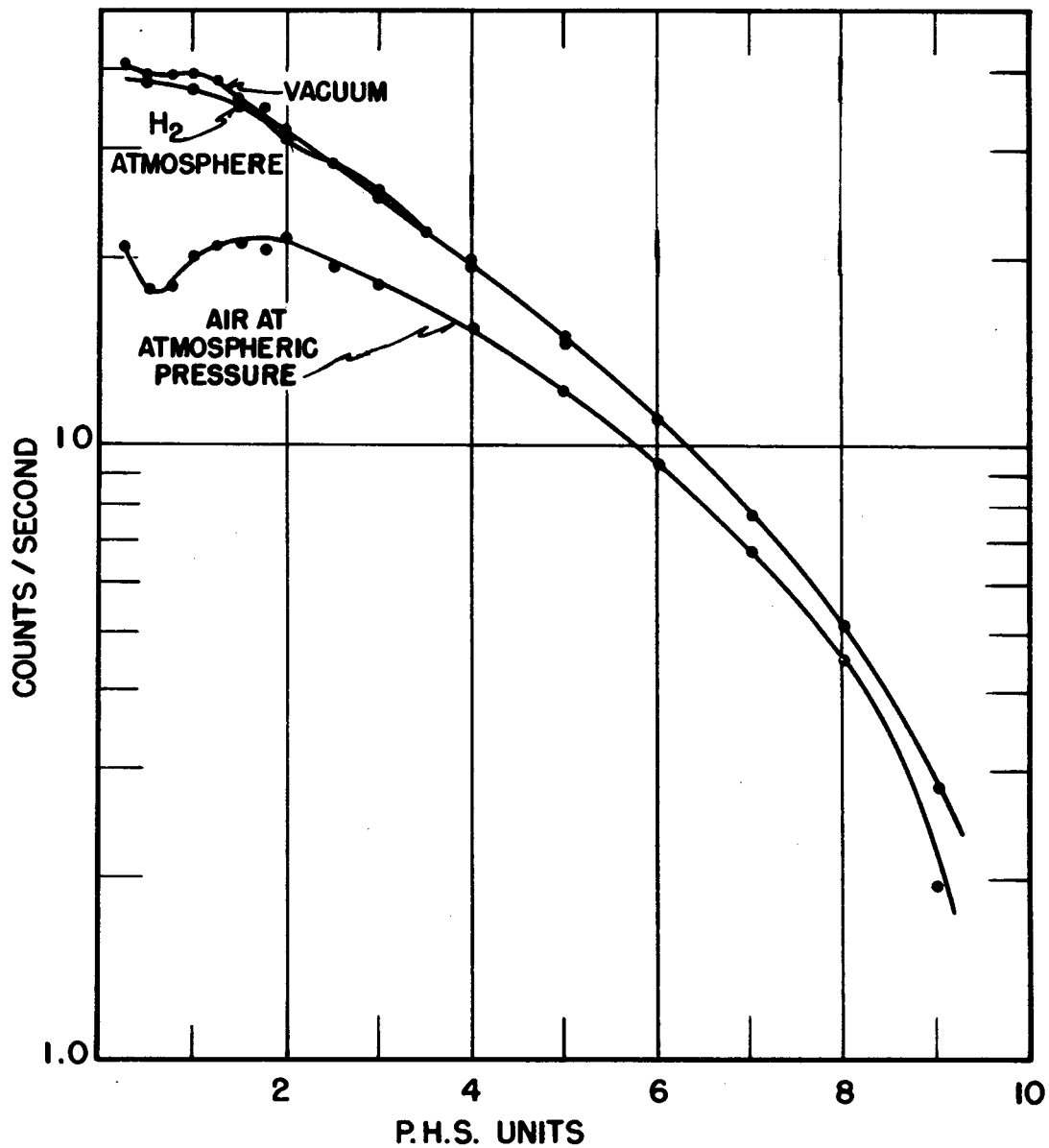


Fig. 14 -  $\text{Ca}^{45}$  Collimated by .030-in. Copper Sheet on Hollow Anthracene Spectrometer.

UNCLASSIFIED

# UNCLASSIFIED

## PHYSICS DIVISION QUARTERLY REPORT

UNCLASSIFIED  
DWG. 10827 R1

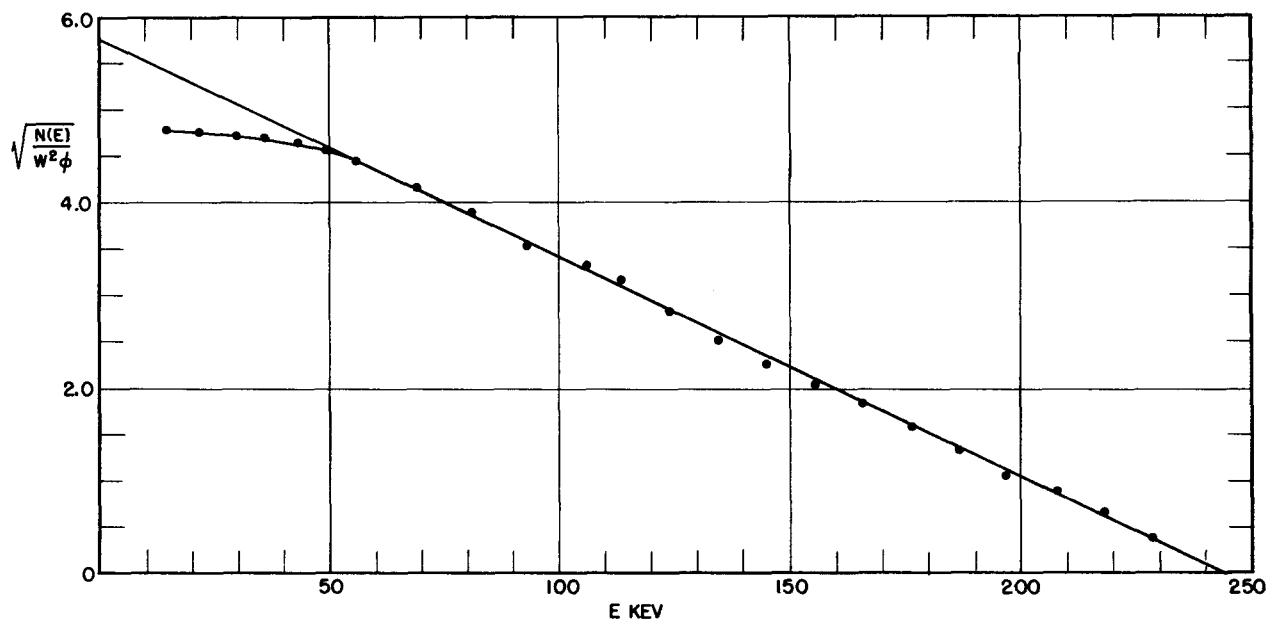


Fig. 15 - Kurie Plot of  $Ca^{45}$  Using Copper Collimator on Hollow Anthracene Spectrometer.

strong absorption dip in an important region for the light from sodium iodide. This sample was a 10% solution of Canada balsam in xylene and was 1 cm in thickness, equivalent to 1 mm of Canada balsam. In using Canada balsam layers of various thicknesses between the sodium iodide crystal and the photomultiplier, a considerable change in resolution was actually observed, there being an optimum thickness for the best resolution.

It appears that a filter constructed of a material having a sharper cut-off than Canada balsam would thus improve the resolution of sodium iodide if inserted in the proper amount between the crystal and the photomultiplier. A substance which appeared to be a possible filter for the light from sodium iodide is a saturated solution

of potassium nitrate. The curve for it is shown in Fig. 17. This curve is extremely steep and cuts off near the low-frequency edge of the absorption shelf in the sodium iodide.

It was observed that several samples of lucite being used for light pipers for these crystals differed in their performance with the crystal and samples of ultraviolet transmitting lucite and ultraviolet absorbing lucite were run as shown in Fig. 17. Some of the ultraviolet absorbing lucites have quite different absorption curves than others. This particular one cuts off at approximately the correct place. The ultraviolet absorption of mineral oil (see Fig. 16) and Dow-Corning 200 make them quite satisfactory liquids to join the sodium iodide crystal to

FOR PERIOD ENDING JUNE 20, 1951

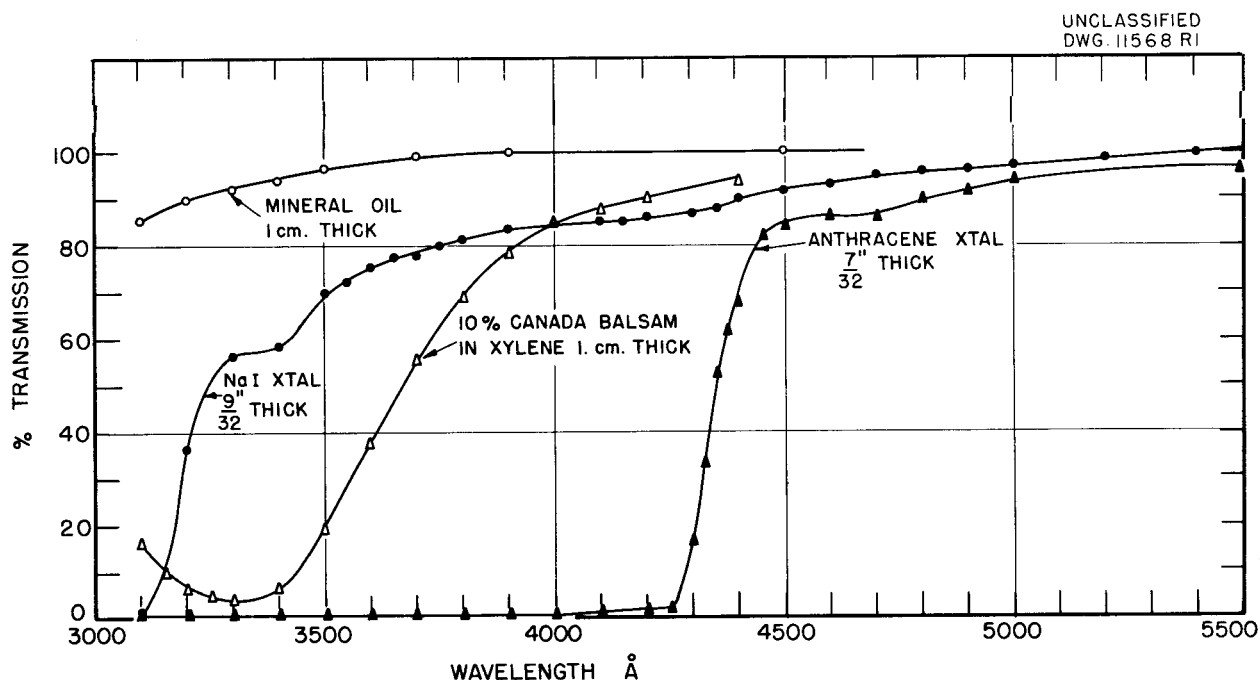


Fig. 16 - Transmission Spectra of Substances Used in Scintillation Spectrometry.

the light piper. Poly- $\alpha$ -methyl styrene was also measured and found to absorb considerably near the short wavelength end of the sodium iodide emission spectrum.

The absorption curves for other scintillation phosphors were measured. *p*-Terphenyl in a solid clear crystal, *p*-terphenyl in *m*-xylene, and a clear trans-stilbene crystal were also measured and their curves are shown in Fig. 17. Solid *p*-terphenyl seems to show some absorption far from its sharp cut-off and solid trans-stilbene shows an absorption step of considerable depth near its cut-off. The fluorescent light from these materials has not been measured well enough to ascertain the effect upon the scintillations as yet. Some measurements of the emitted light from sodium iodide and anthracene have been made in the Chemistry Division

by J. A. Ghormley. These measurements, after being corrected for the transmission of the spectrometer on which they are made, are reproduced here in Fig. 18. These curves are not the true curves of the emitted light since the entire crystal is illuminated in each case and the fluorescent light was partially absorbed in the crystal. Had the crystals been illuminated on one face so that the light would be completely absorbed or completely unabsorbed by the crystal material, they could be directly interpreted. Further measurements of this type would be extremely helpful and should be done. It can be seen that the short wavelength side of the anthracene emission curve coincides with the sharp absorption edge in the solid material. Should a similar condition be obtained with trans-stilbene, this would account

# UNCLASSIFIED

## PHYSICS DIVISION QUARTERLY REPORT

UNCLASSIFIED  
DWG. 11569 RI

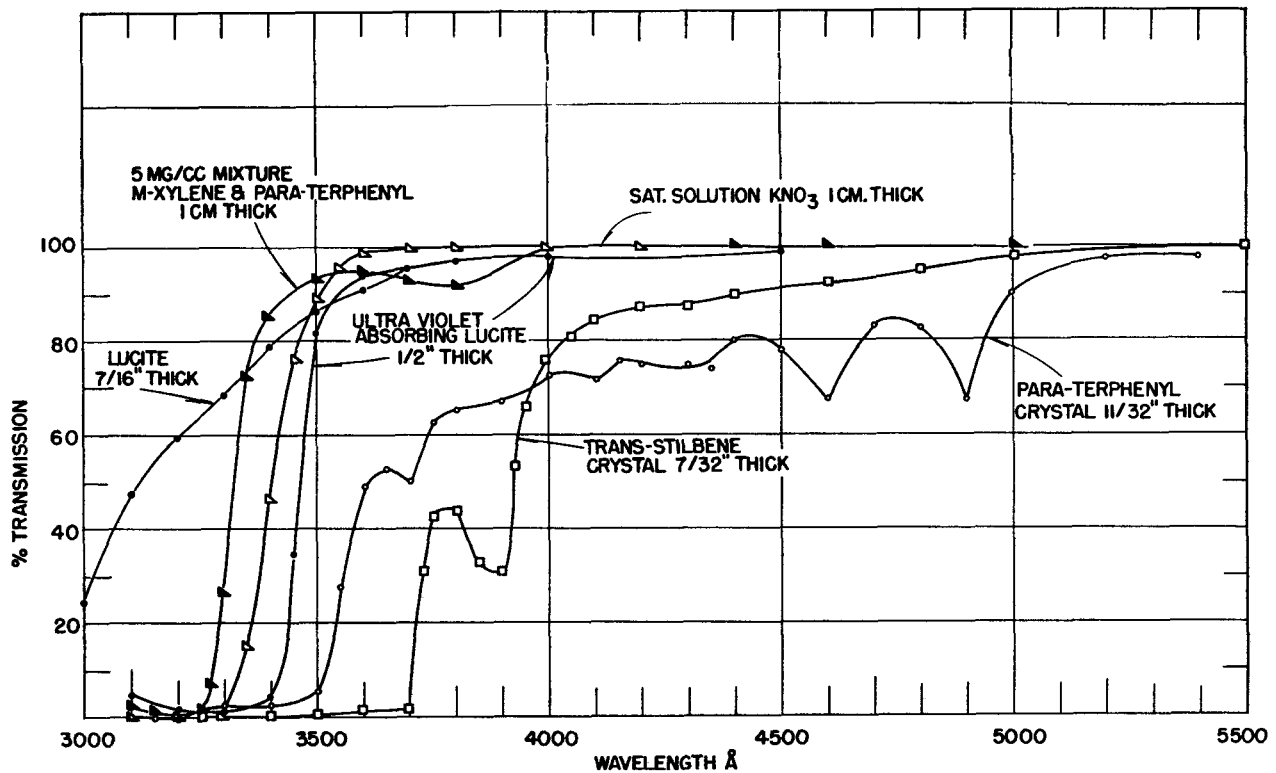


Fig. 17 - Transmission Spectra of Various Crystals and Solutions.

for the poor energy resolution always obtained with good crystals of trans-stilbene.

The energy resolution of sodium iodide scintillation counters has been considerably improved by optical treatment of the crystal and the reflector. It was found that the previously used solvent-polishing method using alcohol or acetone was producing an ultraviolet absorbing layer on the surface of the sodium iodide crystals. By removing these layers by abrasion, in essence preparing the crystals only by grinding

in extremely dry conditions in a dry box, the resolution was very much improved. A crystal which on solvent polishing gave a peak-to-valley ratio of approximately 10 with the 0.661-Mev  $\gamma$  ray of  $\text{Cs}^{137}$  was improved to give a ratio of approximately 25 merely by grinding and dry-polishing the surface. The resolution of a highly polished crystal was much improved by grinding the entire outside with 320 Carborundum. The ratio was decreased again merely by wetting the surfaces with mineral oil, thus restoring some degree of polish.

# UNCLASSIFIED

FOR PERIOD ENDING JUNE 20, 1951

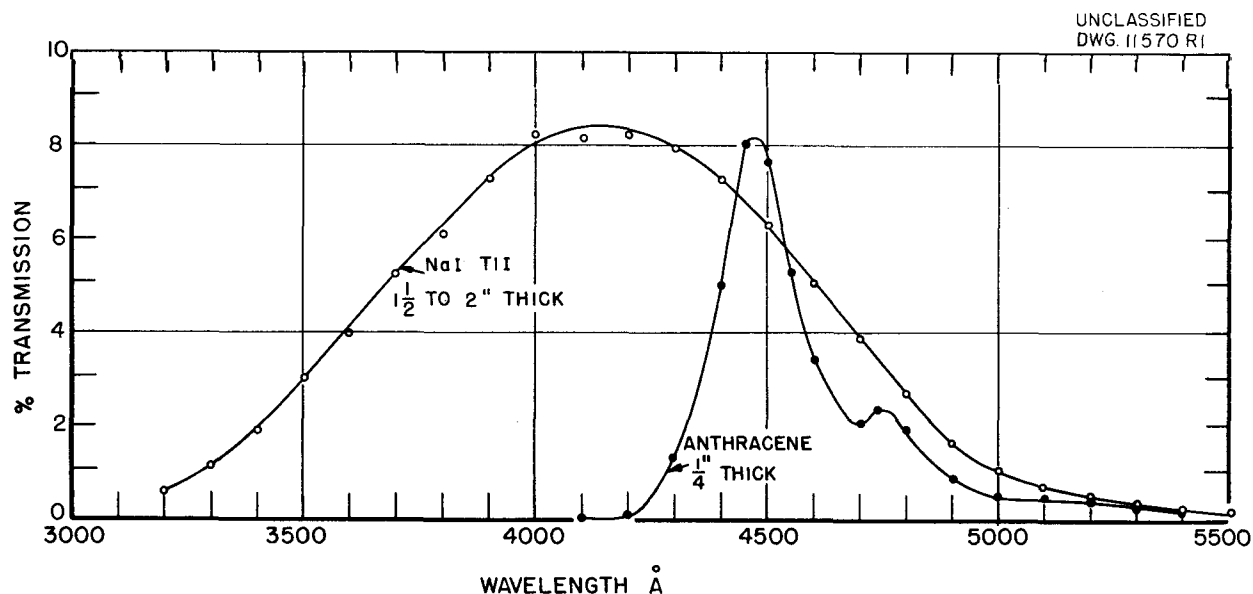


Fig. 18 - Emission Spectra of Anthracene and Sodium Iodide Activated with Thallium.

The ratio was also much improved by surrounding the crystal with highly polished aluminum foil which produced a better reflecting surface than the polish put upon the aluminum container by the shops. With such an arrangement the peak-to-valley ratio on  $\text{Cs}^{137}$  has exceeded 40. The resolution obtained with this ratio is between 8 and 9 percent for the full width at half maximum of the cesium peak at 661 Kev. To obtain these high ratios, the voltage ratio between the photocathode and the dynodes of the photomultiplier must be adjusted. The voltage ratios giving the best result appear to be 5.0, 0.85, 1.2, 1, 1, 1, etc., starting with the photocathode. When a high peak-to-valley ratio was obtained it was observed that there appeared to be an optimum total photomultiplier volt-

age. The ratio of 37 obtained with the total photomultiplier voltage of 620 volts was reduced to 19 by raising the total voltage to 860 volts. This ratio could be restored to 37 by defocussing dynode 6 or 7. This appears to be a saturation or space charge limiting effect in the photomultiplier. The peak current in the photomultiplier for the sodium iodide pulses at which saturation appears to begin is approximately  $30 \mu\text{a}$ . The sodium iodide was replaced with an anthracene crystal whose pulse duration is approximately 10 times shorter; it was then found that a pulse 10 times smaller must be obtained from the photomultiplier before the maximum resolution was obtained, further confirming the belief that this is space charge limitation. Because of the low peak current at

# UNCLASSIFIED

## PHYSICS DIVISION QUARTERLY REPORT

which it occurs, further work is being done to make sure this is a space charge limiting effect.

### HIGH-SPEED SYNCHROSCOPE

G. G. Kelley and R. R. Hall

A new synchroscope is in the process of development for the study of circuits and components to be used in very fast counting equipment and for the investigation of various discharge phenomena. The instrument will be at least five times as fast as the one developed here previously.<sup>(2)</sup>

It is intended that the vertical amplifiers used will have a rise time of about  $1\text{ m}\mu\text{sec}$ . This figure is certainly within a factor of 2 of the fastest response that can be achieved with presently available tubes and to this extent represents a compromise with expediency. A low-frequency analog distributed amplifier has been constructed and studied as an aid to design. It is a 10-tube stage with parasitic grid and plate capacities increased to  $950\ \mu\mu\text{f}$  and uses Miller 0.5-mh choke coils as the half-section inductive elements. These have been disassembled and coupled together in pairs to give the required value of negative mutual inductance for an "m derived" line with  $m = 1.27$ . By calculation  $R_0$ , the low-frequency impedance of the line, is 1.16 K-ohms. The best value determined experimentally is 1.21 K-ohms. This analog circuit has demonstrated that with an optimum "m derived" line in grid and plate circuits, the rise time is equal within 10% to twice the calculated (and measured) delay per section (approximate mean value of the delay in the pass

band is  $1.265\sqrt{LC}$ ) or  $t_{\text{rise}} = 2.54\sqrt{LC} = 2.0 R_0 C'$  where  $L$  and  $C$  are the equivalent full-section "constant  $k$ " impedances,  $R_0$  is the low-frequency impedance of the line, and  $C'$  is the actual circuit shunt capacity ( $C' = mC$ ).

The measured delay per section of the analog amplifier is  $1.15\ \mu\text{sec}$ , and the rise time of the 10-tube stage is  $2.3\ \mu\text{sec}$  when terminated with a "constant  $k$ " half section of the same impedance and cut-off frequency. The rise time increases very slowly as the number of tubes in a stage is increased. It is only a few percent greater in the 10-tube stage than when only half the tubes are used. The overshoot, however, does increase significantly as the tubes per stage are increased. It is about 4% at the unterminated output of a 10-tube stage and appears to increase about 0.4% per tube. Very much improvement can be made by phase correcting condensers from grid to grid. The overshoot has been decreased to less than 1% by this means. It has been found experimentally from the analog that when the grid line is driven from a current generator, whose parasitic capacity equals the line shunt capacity, best pulse fidelity is obtained if the current is applied directly at the mid-series point of the first section of this line. Best open circuit plate line terminations is a "constant  $k$ " half section of equal impedance and cut-off frequency. The standard practice of using an "m derived" half section with  $m = 0.6$  followed by a resistor equal to the low-frequency impedance of this line provides a very good termination with regard to pulse reflection.

### BLUE GLOW FROM LITR

W. H. Jordan

When the first uranium slugs were discharged from the graphite reactor

<sup>(2)</sup>G. G. Kelley, "A High Speed Synchroscope," *Rev. Sci. Instruments* 21, p. 71 (1950).

# UNCLASSIFIED

FOR PERIOD ENDING JUNE 20, 1951

into the canal it was observed that a bluish white light was emitted from the water immediately surrounding the slugs. Since that time there has been much speculation as to the nature of this blue glow. It has usually been attributed to fluorescence in the water due to the action of the  $\gamma$  rays; however, Dr. Phillip Morrison, for one, suggested that Cerenkov radiation might be the cause. Conditions are particularly favorable for viewing this blue glow in the Low Intensity Training Reactor (LITR) since the fuel elements are operated in a tank of water and can readily be viewed through a manhole on the top of the tank. A brief investigation of this radiation has recently been undertaken, and it is now believed that the glow is indeed Cerenkov radiation. The following arguments in support of this view are presented.

First, a few words concerning the nature of Cerenkov radiation. It was first observed by the Russian physicist, P. A. Cerenkov, in 1934; an explanation of the effect based on classical electrodynamics was presented by Frank and Tamm in 1937. The predictions of the theory have been verified by experimental investigation carried out in this country and abroad. The application of quantum electrodynamics has confirmed the predictions of classical theory.

If a charged particle traverses a dielectric medium with a velocity greater than the velocity of light in the medium (for example, an electron with greater than 260 Kev of kinetic energy in water), a cone of radiation will be given off similar to the bow wave from a ship. A simple Huyghens construction shows that the angle that an element of the cone makes with

the axis (i.e., the path of the particle) is given by

$$\sin \theta = \frac{1}{\beta n},$$

where  $\beta$  is the particle velocity and  $n$  is the index of refraction of the medium. The radiation is polarized with the electric vector along an element of the cone. The spectrum of the radiation is continuous throughout the visible region, increasing in intensity toward the violet end; the ultraviolet limit is determined by absorption in the medium. Approximately 40 photons are emitted as visible radiation for every 2-Mev electron traversing the dielectric medium.

In the original experiments performed by Cerenkov, a collimated beam of  $\gamma$  rays from a radium source irradiated a flask of water. He found that the light emitted from the water had the following properties:

1. It was concentrated in the forward direction.
2. It was partially polarized.
3. It was a continuous spectrum with a maximum in the blue-violet.
4. It was not quenched by addition of potassium iodide, a known fluorescence quencher.
5. The radiation was not emitted when the water was irradiated with 30-Kev X rays.

These results were confirmed in this country by Collins and Reiling using monoenergetic electrons. They found the radiation was confined to a cone at the predicted angle. The light was described as bluish white, the spectrum showing no signs of structure.

From the above experiments one would predict that a reactor operated in a

UNCLASSIFIED

# UNCLASSIFIED

## PHYSICS DIVISION QUARTERLY REPORT

tank of water should give off a bluish-white light due to Cerenkov radiation. Most of the experiments that one could perform would serve only to confirm the experimental results of Cerenkov. Nevertheless, a few observations have been made. The glow from the reactor has been observed with a hand spectroscope, and a continuous spectrum was seen. There was no sign of band structure with the admittedly low resolution obtainable.

One would not expect the radiation to be strongly polarized because the source is large compared to the distance from the reactor at which radiation can be observed. In addition, the Compton recoil electrons can make a

fairly large angle with the direction of the gamma photons and still be energetic enough to excite Cerenkov radiation. Nevertheless an observation of the glow from the sides of the reactor shows a small amount of polarization with the electric vector along a radius from the reactor center. What one actually observes is a minimum in the light transmitted by a piece of polaroid when it is oriented as to exclude radiation that is polarized with the electric vector perpendicular to the reactor face.

The above considerations indicate that the blue glow observed in the reactor and from irradiated slugs in the canal is due to Cerenkov radiation.

# UNCLASSIFIED

FOR PERIOD ENDING JUNE 20, 1951

## 9. THEORETICAL PHYSICS

A large part of the unclassified work of the theoretical physics group in recent months has been concerned with theoretical problems of nuclear spectroscopy: internal conversion, angular correlation of nuclear radiations, and  $\beta$  decay. In addition, progress has been made on theoretical problems connected with nuclear alignment and scattering. The latter has application to the radiation damage investigation. The following is a brief description of the nature and status of current problems.

### L-SHELL INTERNAL CONVERSION

M. E. Rose

The calculation of L-shell internal conversion coefficients is being carried out in Washington on the Bureau of Standards machine (SEAC). The conversion coefficients are calculated in a completely relativistic way, and the effects of screening are included. The work also includes calculation of low-energy K-shell coefficients in the same manner. The range of parameters is  $5 \leq Z \leq 95$  (in steps of 10), transition energy between about 25 Kev and 1 Mev (10 values), and 10 multipoles. Complete results should be available sometime near the end of the summer.

### ANGULAR CORRELATION WITH CONVERSION ELECTRONS

M. E. Rose and G. B. Arfken

The K-shell conversion calculation provided numerical values of matrix

elements which can be used to find the angular correlation of any double cascade in which one or both transitions are conversion processes. A method has been found to relate the angular distribution function for conversion electrons to that of  $\gamma$  rays. Thus, the angular distribution of conversion electrons can be found for all dipole and quadrupole transitions and for all (practical) higher multipoles in which the angular momentum is the smallest value allowed by the conservation of angular momentum. This makes use of published  $\gamma$ -ray distribution functions.<sup>(1)</sup> Then, using further published results,<sup>(2)</sup> we can obtain the correlation for conversion electrons (c.e.) with  $\gamma$  rays,  $\alpha$  particles,  $\beta$  particles, and also the c.e.-c.e. correlation. The latter depends on the fact that after one electron has been ejected the K shell will always be filled very rapidly before the second conversion takes place. Numerical results are available now for dipole and quadrupole transitions.

### POLARIZATION OF CAPTURE GAMMA RADIATION

G. B. Arfken                      M. E. Rose  
L. C. Biedenharn

In a previous report<sup>(2)</sup> it was shown that when polarized s-neutrons are captured by a nucleus the resultant  $\gamma$  rays are isotropic even when observed

---

(1) D. L. Falkoff and G. E. Uhlenbeck, "On the Directional Correlation of Successive Nuclear Radiations," *Phys. Rev.* 79, 323 (1950); S. Lloyd, *Phys. Rev.* (to be published).

(2) L. C. Biedenharn, M. E. Rose, and G. B. Arfken, *Can Polarization Effects Be Detected in Capture Gamma Radiation?*, ORNL-986 (Mar. 26, 1951).

UNCLASSIFIED

# UNCLASSIFIED

## PHYSICS DIVISION QUARTERLY REPORT

with a (linear) polarization-sensitive detector. This is also true for mixed (electric and magnetic) radiation. If, however, the detector can discriminate between left and right circular polarization one would observe anisotropy, the measurement of which would give information concerning the multipolarity of the emitted  $\gamma$ 's and the angular momentum of the levels involved. We have calculated the anisotropy of the circularly polarized photons. For a quarter wave plate it is proposed to use Compton scattering from magnetized iron. An investigation has been begun for the purpose of evaluating completely and carefully the optimum conditions for the experiment, taking into account finite solid angles and other geometrical factors. A Letter to the Editor has been submitted for publication in *The Physical Review*.

### ISOTROPY OF NUCLEAR GAMMA RADIATION

G. B. Arfken                      M. E. Rose  
L. C. Biedenharn

The  $B^{11}(p, \gamma)C^{12}$  experiments, in which the angular distribution of the cross-over and cascade gammas relative to the  $p$ -proton beam is measured, can be explained only if one postulates two levels in the compound nucleus  $C^{12}$  which are reached when the protons are captured. This is based on the observation that cross-over is isotropic, and the first gamma in the cascade is not. It has been demonstrated, in general, that if a  $2^L$  pole  $\gamma$  is emitted isotropically and  $L \geq J - \frac{1}{2}$ , where  $J$  is the angular momentum of the emitting level, then all gamma radiation from this level must be isotropic. Actually the proof depends on some laborious calculations which have been carried out for dipole, quadrupole, and octupole

radiation. Also, the result does not apply in certain isolated cases. These are  $3/2 \longrightarrow 3/2$  and  $5 \longrightarrow 4$  with quadrupole emission. None of these exceptions are pertinent for the reaction cited. A manuscript has been submitted for publication in *The Physical Review*.

### ANGULAR CORRELATION IN BETA DECAY

G. B. Arfken                      M. E. Rose  
L. C. Biedenharn

The  $\beta$ - $x$  angular correlation, where  $x$  is any radiation, depends on the calculation of the angular distribution of  $\beta$  particles when the nuclear transition corresponds to a fixed change in the orientation of the nuclear angular momentum. This was considered in the  $Z = 0$  approximation by Falkoff and Uhlenbeck.<sup>(1)</sup> Work is now in progress to extend these results by including the Coulomb field. The procedure is, of course, to use the angular momentum representation for the  $\beta$  particle, and it is believed that this has certain advantages in any case (even for  $Z = 0$ ) so far as an understanding of the results is concerned.

### THE GENERAL BETA-DECAY INTERACTION

L. C. Biedenharn and M. E. Rose

The most general  $\beta$ -decay interaction is a linear combination of five well-known invariant interactions. As an outgrowth of certain questions in  $\beta$  decay it has been possible to show that the constants have the same phase and may all be taken as real. The de Groot-Tolhoek<sup>(3)</sup> symmetry principle

(3) H. A. Tolhoek and S. R. de Groot, *Physica* 16, 456 (1950).

# UNCLASSIFIED

FOR PERIOD ENDING JUNE 20, 1951

is shown to be unique. These considerations form the basis of a publication to appear shortly in *The Physical Review*.

## EFFECT OF FINITE SIZE OF NUCLEUS IN BETA DECAY

M. E. Rose and D. K. Holmes

It has not been possible to fit the RaE spectrum, but the result that the finite nuclear size has an appreciable effect in forbidden (parity not favorable) transitions is of interest. A Letter to the Editor will appear shortly in *The Physical Review*.

## NUCLEAR ALIGNMENT

M. E. Rose and A. Simon

The expression given by Rose (AECD-2119) for the nuclear alignment produced by HFS coupling with external magnetic field would seem to be based on the neglect of off-diagonal elements of the HFS (A I·S) in the strong field representation. This expression can be shown to have a very general validity involving only the requirement that  $A/kt \ll 1$  and being valid for arbitrary crystalline fields as well as for the assumption of dipole-dipole couplings between the ions. This last result assures us that dilution will not destroy nuclear alignment because of a broadening of the energy levels [contrary to a statement by Bleaney, *Phil. Mag.* 42, 441 (1951)] and that its effect can be controlled by a proper choice of sample shape as follows from the work of Van Vleck [*J. Chem. Phys.* 5, 300 (1937)]. A communication on this subject has been submitted to *The Philosophical Magazine (London)*.

## ON THE STOPPING POWER FOR FISSION FRAGMENTS

S. Tamor

The effect of the screening by the orbital electrons on the slowing down of fission fragments has been investigated. It is usually assumed that the stopping cross-section for an ion is that of a proton of the same velocity times the square of the ionic charge.<sup>(4)</sup> An estimate of the contribution to the stopping of the inner core of the ion may be made by considering the hypothetical case of the slowing down of a neutron atom with rigidly bound electrons. For reasonable values of the screening radius, the stopping cross-section turns out to be almost equal to that of the bare nucleus (to within a factor of 2 or 3), in spite of the fact that the total ionic charge is zero. This arises from the fact that most of the energy loss comes from very close collisions in which the screening is unimportant.

This result seems, therefore, contrary to the assumption in reference (4) that the stopping cross-section of a fission fragment is a poor measure of its ionic charge.

## TABULATION OF THE RACAH COEFFICIENTS

C. Perry            M. Rankin  
L. C. Biedenharn

The Racah coefficients,<sup>(5)</sup>

$$W(l_1 J_1 \ l_2 J_2; sL),$$

(4) J. Knipp and E. Teller, "On the Energy Loss of Heavy Ions," *Phys. Rev.* 59, 659 (1941).

(5) G. Racah, "Theory of Complex Spectra. II," *Phys. Rev.* 62, 438 (1942).

UNCLASSIFIED

# UNCLASSIFIED

## PHYSICS DIVISION QUARTERLY REPORT

have recently been shown to be of interest in the angular distributions in nuclear reactions.<sup>(6)</sup> A tabulation of these coefficients [and the related quantities

$$Z(l_1 J_1 \ l_2 J_2; \ sL)$$

of reference (6)] has therefore been undertaken. The general formula for the  $W$ 's has been given by Racah.<sup>(5)</sup> For calculational purposes, it was found useful first to tabulate the Racah coefficients as algebraic functions,<sup>(7)</sup> similar to the well-known tabulations of the vector addition coefficients. In order to further simplify the numerical work, recursion formulas for the  $W$ 's have been developed. The most general of these, which may be of intrinsic interest, is

$$W(aa \ b\beta; \ c\gamma) \ W(\bar{a}\alpha \ \bar{b}\beta; \ \bar{c}\gamma)$$

$$= \sum_{\delta} (2\delta + 1) \ W(\bar{a}\delta \ \alpha c; \ \bar{a}\bar{c}) \ W(b\delta \ \beta\bar{c}; \ \bar{b}\bar{c}) \cdot W(\bar{a}\delta \ \gamma b; \ \bar{a}\bar{b}) \ . \quad (1)$$

The present work will comprise the (numerical) tabulation of

$$W(l_1 J_1 \ l_2 J_2; \ sL)$$

and

$$Z(l_1 J_1 \ l_2 J_2; \ sL)$$

(6) J. M. Blatt and L. C. Biedenharn, "The Angular Dependence of Scattering and Reaction Cross Sections," *Phys. Rev.* 82, 123 (1951).

(7) H. A. Jahn ["Theoretical Studies in Nuclear Structure. II," *Proc. Roy. Soc. (London)* A205, p. 192, esp. p. 233 (1951)] has also done this (for  $s = 0, \frac{1}{2}, \dots, 2$ ).

for the following range of values:

$$s = 0, \frac{1}{2}, \dots, 3$$

$$L = 0, 1, \dots, 8$$

$$l_1, l_2 = 0, 1, \dots, 4$$

$$J_1, J_2 = 0, \frac{1}{2}, \dots, 4$$

Currently we have completed the tables for  $s = 0, \frac{1}{2}, \dots, 2$  with the values previously listed for the other variables.

## THE TRIPLET FORCE BETWEEN LIKE NUCLEONS

F. G. Prohammer and T. A. Welton

The present information on nuclear forces is very sketchy. The singlet

---

potentials between two protons and between a neutron and a proton are known to the extent of two parameters (scattering length and effective range). These potentials are attractive and seem to be approximately the same. The mirror nuclei evidence strongly suggests that the neutron-neutron force is very nearly the same as the proton-proton force. Two parameters are likewise known for the neutron-proton triplet potential, which appears to be considerably more attractive than the singlet potential. No information exists, however, on the triplet like-particle potential. This must be

# UNCLASSIFIED

FOR PERIOD ENDING JUNE 20, 1951

assumed the same between two neutrons as between two protons, because of the mirror nuclei evidence.

All the available information comes from the study of two particle states of zero orbital angular momentum, and various plausible exchange characters have been devised for the forces in order to describe states of greater complexity. The Majorana exchange force was designed to yield saturation at the  $\alpha$  particle, an essential requirement. The Berkeley evidence, however, is that the  $n$ - $p$  force is not sufficiently of Majorana type to yield saturation. Qualitatively correct saturation properties, however, can be achieved in a different manner. Assume no correction between the triplet  $n$ - $p$  potential and the triplet  $p$ - $p$  and  $n$ - $n$  potentials. The Berkeley evidence is that the  $n$ - $p$  potential is never repulsive, no matter what the space or spin state. The like-particle triplet interaction must then be repulsive in order to yield saturation. It can further be said that this interaction must be strongly repulsive and over a large range,<sup>(8)</sup> since  $\text{He}^5$  and  $\text{Li}^5$  are not bound. This must be so since in  $\text{He}^5$ , for example, the extra neutron is in a triplet state with respect to only one neutron, yet the presumed repulsion is effective in cancelling the other three attractions to prevent binding.

Such a strong repulsion should give striking effects, aside from the saturation. It should show up very clearly in  $p$ - $p$  scattering at 20 or 30 Mev. It further has an important effect in the

(8) This picture must be contrasted with that of R. Jastrow ["On Charge Independence and High Energy Scattering," *Phys. Rev.* 79, 389 (1950)], who assumes a short-range repulsion accompanied by a strong noncentral interaction.

$^4S$  state of the three-body problem, and this effect is being calculated.

It is known that one bound state of  $\text{H}^3$  exists. This is a  $^2S$  state (ignoring small admixtures produced by noncentral forces), and its binding energy is known to follow quite well by calculation. In these calculations potentials are used which have been adjusted to fit the two-body data. The triplet like-particle force does not enter in any important way, so that lack of knowledge concerning it does not seriously affect the calculation.

The situation with the  $^4S$  state is completely different. Two pieces of information are available, first that no such bound state exists, and second that the value of the scattering length for slow neutrons incident on deuterons is a  $^4S$  state. For this state the triplet like-particle force is all-important, since the wave equation is

$$-\frac{\hbar^2}{2M} (\nabla_1^2 + \nabla_2^2 + \nabla_3^2) \psi + [V(r_{13}) + V(r_{23}) + U(r_{12})] \psi = E\psi. \quad (1)$$

Here  $M$  is the nucleon mass, 1 and 2 are neutrons, and 3 is the proton. The function  $V$  is the triplet neutron-proton potential, while  $U$  is the triplet neutron-neutron potential. The exclusion principle requires that

$$\psi(x_1, x_2, x_3) = -\psi(x_2, x_1, x_3). \quad (2)$$

A conventional variational calculation is in progress for the binding energy  $E$ , using various assumptions

UNCLASSIFIED

# UNCLASSIFIED

## PHYSICS DIVISION QUARTERLY REPORT

for  $U$  and adjusting  $V$  to fit the low-energy data. Potentials of exponential shape are being used, and the trial functions are taken to be products of exponentials in the interdistances, containing three adjustable parameters. The algebraic work is complete, and numerical results will be available shortly, together with a more complete description of the work and references to previous work.

The unknown function  $U$  is first taken to be zero. It is anticipated (but not yet certain) that a bound state will then be obtained. The binding energy is underestimated by the variational method, so this result will mean that  $U$  must certainly be repulsive. Further adjustment of  $U$  should yield some rough information on the magnitude and extent of this repulsion.